

The protonmotive force and respiratory control:

Building blocks of mitochondrial physiology

Part 1.

http://www.mitoeagle.org/index.php/MitoEAGLE_preprint_2017-09-21

Preprint version 07 (2017-10-07)

MitoEAGLE Network

Corresponding author: Gnaiger E

Contributing co-authors

Ahn B, Alves MG, Amati F, Åsander Frostner E, Battino M, Beard DA, Ben-Shachar D, Bishop D, Breton S, Brown GC, Brown RA, Buettner GR, Cervinkova Z, Chicco AJ, Coen PM, Collins JL, Crisóstomo L, Davis MS, Dias T, Distefano G, Doerrier C, Ehinger J, Elmer E, Fell DA, Filipovska A, Fisher J, Garcia-Roves PM, Garcia-Souza LF, Genova ML, Gonzalo H, Goodpaster BH, Gorr TA, Han J, Harrison DK, Hellgren KT, Hernansanz P, Holland O, Hoppel CL, Iglesias-Gonzalez J, Irving BA, Iyer S, Jansen-Dürr P, Jespersen NR, Jha RK, Käämbre T, Kane DA, Kappler L, Keijer J, Komlodi T, Krako Jakovljevic N, Kuang J, Labieniec-Watala M, Lai N, Laner V, Lee HK, Lemieux H, Lerfall J, Lucchinetti E, MacMillan-Crow LA, Makrecka-Kuka M, Meszaros AT, Moiso N, Molina AJA, Montaigne D, Moore AL, Murray AJ, Newsom S, Nozickova K, O'Gorman D, Oliveira PF, Oliveira PJ, Orynbayeva Z, Pak YK, Palmeira CM, Patel HH, Pesta D, Petit PX, Pichaud N, Pirkmajer S, Porter RK, Pranger F, Prochownik EV, Reboredo P, Renner-Sattler K, Robinson MM, Rohlena J, Røslund GV, Rossiter HB, Salvadego D, Scatena R, Schartner M, Scheibye-Knudsen M, Schilling JM, Schlattner U, Schoenfeld P, Scott GR, Singer D, Sobotka O, Spinazzi M, Stocker R, Sumbalova Z, Suravajhala P, Tanaka M, Tandler B, Tepp K, Tomar D, Towheed A, Trivigno C, Tronstad KJ, Tyrrell DJ, Velika B, Vendelin M, Vercesi AE,

27 Victor VM, Ward ML, Watala C, Wei YH, Wieckowski MR, Wohlwend M, Wolff J, Wuest
28 RCI, Zaugg M, Zorzano A

29

30 Supporting co-authors:

31 Arandarčikaitė O, Bailey DM, Bakker BM, Batista Ferreira J, Bernardi P, Boetker HE,
32 Borsheim E, Borutaitė V, Bouitbir J, Calabria E, Calbet JA, Carvalho E, Chaurasia B,
33 Clementi E, Collin A, Das AM, De Palma C, Dubouchaud H, Duchon MR, Durham WJ,
34 Dyrstad SE, Engin AB, Fornaro M, Gan Z, Garlid KD, Garten A, Gourlay CW, Granata C,
35 Haas CB, Haavik J, Haendeler J, Hand SC, Hepple RT, Hickey AJ, Hoel F, Kainulainen H,
36 Keppner G, Khamoui AV, Klingenspor M, Koopman WJH, Kowaltowski AJ, Krajcova A,
37 Lenaz G, Malik A, Markova M, Mazat JP, Menze MA, Methner A, Muntané J, Muntean DM,
38 Neuzil J, Oliveira MT, Pallotta ML, Parajuli N, Pettersen IKN, Pulinilkunnil T, Ropelle ER,
39 Salin K, Sandi C, Sazanov LA, Siewiera K, Silber AM, Skolik R, Smenes BT, Soares FAA,
40 Sokolova I, Sonkar VK, Stankova P, Stier A, Swerdlow RH, Szabo I, Trifunovic A, Thyfault
41 JP, Tretter L, Trougakos IP, Vieyra A, Votion DM, Williams C, Zaugg K

42

43 **Updates:**

44 http://www.mitoeagle.org/index.php/MitoEAGLE_preprint_2017-09-21

45

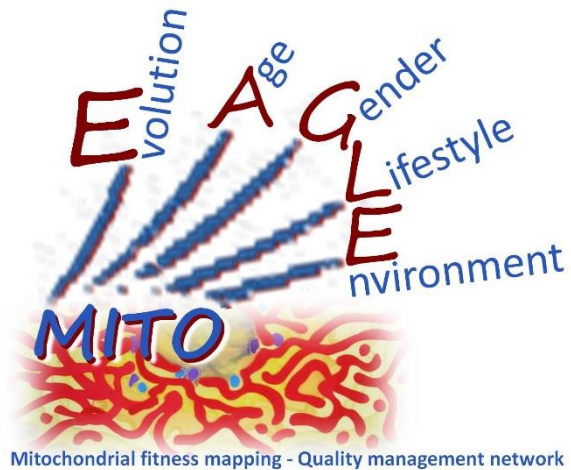
Correspondence: Gnaiger E

Department of Visceral, Transplant and Thoracic Surgery, D. Swarovski Research Laboratory, Medical University of Innsbruck, Innrain 66/4, A-6020 Innsbruck, Austria

Email: erich.gnaiger@i-med.ac.at

Tel: +43 512 566796, Fax: +43 512 566796 20

This manuscript on 'The protonmotive force and respiratory control' is a position statement in the frame of COST Action CA15203 MitoEAGLE. The list of co-authors evolved from MitoEAGLE Working Group Meetings and a **bottom-up** spirit of COST in phase 1: This is an open invitation to scientists and students to join as co-authors, to provide a balanced view on mitochondrial respiratory control, a fundamental introductory presentation of the concept of the protonmotive force, and a consensus statement on reporting data of mitochondrial respiration in terms of metabolic flows and fluxes. We plan a series of follow-up reports by the expanding MitoEAGLE Network, to increase the scope of recommendations on harmonization and facilitate global communication and collaboration.



Phase 2 - until **October 12**: We continue to invite comments and suggestions on the MitoEAGLE preprint, particularly if you are an **early career investigator adding an open future-oriented perspective**, or an **established scientist providing a balanced historical basis**. Your critical input into the quality of the manuscript will be most welcome, improving our aims to be educational, general, consensus-oriented, and practically helpful for students working in mitochondrial respiratory physiology.

To join as a co-author, please feel free to focus on a particular section in terms of direct input and references, contributing to the scope of the manuscript from the perspective of your expertise. Your comments will be largely posted on the discussion page of the MitoEAGLE preprint website.

If you prefer to submit comments in the format of a referee's evaluation rather than a contribution as a co-author, I will be glad to distribute your views to the updated list of co-authors for a balanced response. We would ask for your consent on this open bottom-up policy.

We organize a MitoEAGLE session linked to our series of reports at the MiPconference Nov 2017 in Hradec Kralove in close association with the MiPsociety (where you hopefully will attend) and at EBEC 2018 in Budapest.

» http://www.mitoeagle.org/index.php/MiP2017_Hradec_Kralove_CZ

I thank you in advance for your feedback.

With best wishes,

Erich Gnaiger

Chair Mitochondrial Physiology Society - <http://www.mitophysiology.org>

Chair COST Action MitoEAGLE - <http://www.mitoeagle.org>

Medical University of Innsbruck, Austria

95	Contents
96	1. Introduction
97	2. Respiratory coupling states in mitochondrial preparations
98	Mitochondrial preparations
99	2.1. <i>Three coupling states of mitochondrial preparations and residual oxygen consumption</i>
100	Coupling control states
101	Respiratory capacities and kinetic control
102	Phosphorylation, P _o
103	LEAK, OXPHOS, ET, ROX
104	2.2. <i>Coupling states and respiratory rates</i>
105	2.3. <i>Classical terminology for isolated mitochondria</i>
106	States 1-5
107	3. The protonmotive force and proton flux
108	3.1. <i>Electric and chemical partial forces versus electrical and chemical units</i>
109	Faraday constant
110	Electrical part of the protonmotive force
111	Chemical part of the protonmotive force
112	3.2. <i>Definitions</i>
113	Control and regulation
114	Respiratory control and response
115	Respiratory coupling control
116	Pathway control states
117	The steady-state
118	3.3. <i>Forces and fluxes in physics and irreversible thermodynamics</i>
119	Vectorial and scalar forces, and fluxes
120	Coupling
121	Coupled versus bound processes
122	4. Normalization: fluxes and flows
123	4.1. <i>Flux per chamber volume</i>
124	4.2. <i>System-specific and sample-specific normalization</i>
125	Extensive quantities
126	Size-specific quantities
127	Molar quantities
128	Flow per system, I
129	Size-specific flux, J
130	Sample concentration, C_{mX}
131	Mass-specific flux, J_{mX,O_2}
132	Number concentration, C_{NX}
133	Flow per sample entity, I_{X,O_2}
134	4.3. <i>Normalization for mitochondrial content</i>
135	Mitochondrial concentration, C_{mte} , and mitochondrial markers
136	Mitochondria-specific flux, J_{mte,O_2}
137	4.4. <i>Conversion: units and normalization</i>
138	4.5. <i>Conversion: oxygen, proton and ATP flux</i>
139	5. Conclusions
140	6. References
141	

142 **Abstract**

143 Clarity of concepts and consistency of nomenclature are trademarks of a research field across
144 its specializations, facilitating transdisciplinary communication and education. As research and
145 knowledge of mitochondrial physiology expand, the necessity for harmonizing nomenclature
146 concerning mitochondrial respiratory states and rates has become apparent. Peter Mitchell's
147 concept of the protonmotive force establishes the links between electrical and chemical
148 components of energy transformation and coupling in oxidative phosphorylation. This unifying
149 concept provides the framework for developing a consistent terminology of mitochondrial
150 physiology and bioenergetics. We follow IUPAC guidelines on general terms of physical
151 chemistry, extended by concepts of open systems and irreversible thermodynamics. We align
152 the nomenclature of classical bioenergetics on respiratory states with a concept-driven
153 constructive terminology to address the meaning of each respiratory state. Standards for
154 evaluation of respiratory states must be followed for the development of databases of
155 mitochondrial respiratory function in species, tissues and cells studied under diverse
156 physiological and experimental conditions.

157

158 *Keywords:* Mitochondrial respiratory control, coupling control, mitochondrial
159 preparations, protonmotive force, chemiosmotic theory, oxidative phosphorylation, OXPHOS,
160 efficiency, electron transfer, ET; proton leak, LEAK, residual oxygen consumption, ROX, State
161 2, State 3, State 4, normalization, flow, flux

162

163

Box 1:

164

165

166

167

168

**In brief:
mitochondria
and Bioblasts**

- * Does the public expect biologists to understand Darwin's theory of evolution?
- * Do students expect that researchers of bioenergetics can explain Mitchell's theory of chemiosmotic energy transformation?

169

170

171

172

173

174

175

176

177

178

179

180

181

182

183

184

185

186

187

188

189

190

Mitochondria are dynamic organelles contained within eukaryotic cells, with a double membrane. The inner mitochondrial membrane shows dynamic tubular and disk-shaped cristae that separate the mitochondrial matrix, *i.e.* the internal mitochondrial compartment, and the intermembrane space; the latter being enclosed by the outer mitochondrial membrane. Mitochondria were described for the first time in 1857 by Rudolph Albert von Kölliker as granular structures or ‘sarkosomes’. In 1886 Richard Altmann called them ‘bioblasts’ (published 1894). The word ‘mitochondrium’ (Greek mitos: thread; chondros: granule) was introduced by Carl Benda (1898). Mitochondria are the oxygen consuming electrochemical generators which evolved from endosymbiotic bacteria (Margulis 1970). The bioblasts of Richard Altmann (1894) include not only the mitochondria, but also symbiotic and free-living bacteria. Mitochondria are the structural and functional elemental units of cell respiration, where cell respiration is defined as the consumption of oxygen coupled to electrochemical proton translocation across the inner mitochondrial membrane. In the process of oxidative phosphorylation (OXPHOS), the reduction of O₂ is electrochemically coupled to conservation of energy in the form of ATP (Mitchell 2011). These powerhouses of the cell contain the machinery of the OXPHOS pathway, including transmembrane respiratory complexes (*i.e.* FMN, Fe-S and cytochrome *b*, *c*, *aa*₃ redox systems), alternative dehydrogenases and oxidases, the coenzyme ubiquinone (coenzyme Q) and ATP synthase together with the enzymes of the tricarboxylic acid cycle and the fatty acid oxidation enzymes, ion transporters, including substrate, co-factor and metabolite transporters as well as proton pumps, and mitochondrial kinases related to energy transfer pathways. The mitochondrial proteome comprises over 1,200 proteins (Mitocharta), mostly encoded by nuclear DNA (nDNA), with a variety of functions,

191 many of which are relatively well known (*e.g.* apoptosis-regulating proteins), are still under
192 investigation, or need to be identified (alanine transporter). Mitochondria typically maintain
193 several copies of their own genome (hundred to thousands per cell) which is maternally
194 inherited and known as mitochondrial DNA (mtDNA). One exception to strictly maternal
195 inheritance in animals is found in bivalves (Breton *et al.* 2007). mtDNA is 16.5 Kb in length,
196 contains 13 protein-coding genes for subunits of the transmembrane respiratory Complexes CI,
197 CIII, CIV and ATP synthase, and also encodes 22 tRNAs and the mitochondrial 16S and 12S
198 rRNA. The mitochondrial genome is both regulated and supplemented by nuclear-encoded
199 mitochondrial targeted proteins. Evidence has accumulated that additional gene content is
200 encoded in the mitochondrial genome, *e.g.* microRNAs, piRNA, smithRNAs, repeat associated
201 RNA, and even additional proteins. The inner mitochondrial membrane contains the non-
202 bilayer phospholipid cardiolipin, which is not present in any other eukaryotic cellular
203 membrane. Cardiolipin promotes the formation of respiratory supercomplexes, which are
204 supramolecular assemblies based upon specific, though dynamic, interactions between
205 individual respiratory complexes (Lenaz *et al.* 2017). There is a constant crosstalk between
206 mitochondria and the other cellular components at the transcriptional or post-translational level,
207 and through cell signalling in response to varying energy demands (Quiros *et al.* 2016). In
208 addition to mitochondrial movement along the microtubules, mitochondrial morphology can
209 change in response to energy requirements of the cell via processes known as fusion and fission
210 through which mitochondria can communicate within a network, and in various pathological
211 states which cause swelling or dysregulation of fission and fusion. Mitochondrial dysfunction
212 is associated with a wide variety of genetic and degenerative diseases. Therefore, a better
213 understanding of mitochondrial physiology will improve our understanding of the etiology of
214 disease and the diagnostic repertoire of mitochondrial medicine. Abbreviation: mt, as generally
215 used in mtDNA. Mitochondrion is singular and mitochondria is plural.

216 *‘For the physiologist, mitochondria afforded the first opportunity for an experimental*
217 *approach to structure-function relationships, in particular those involved in active transport,*
218 *vectorial metabolism, and metabolic control mechanisms on a subcellular level’ (Ernster and*
219 *Schatz 1981).*

220

221 **1. Introduction**

222 Mitochondria are the powerhouses of the cell with numerous physiological, molecular,
223 and genetic functions (**Box 1**). Every study of mitochondrial function and disease is faced with
224 **E**volution, **A**ge, **G**ender and sex, **L**ifestyle, and **E**nvironment (EAGLE) as essential background
225 conditions characterizing the individual patient or subject, cohort, species, tissue and to some
226 extent even cell line. As a large and highly coordinated group of laboratories and researchers,
227 the global MitoEAGLE Network’s mission is to generate the necessary scale, type, and quality
228 of consistent data sets and conditions to address this intrinsic complexity. Harmonization of
229 experimental protocols and implementation of a quality control and data management system
230 is required to interrelate results gathered across a spectrum of studies and to generate a
231 rigorously monitored database focused on mitochondrial respiratory function. In this way,
232 researchers within the same and across different disciplines will be positioned to compare their
233 findings to an agreed upon set of clearly defined and accepted international standards.

234 Reliability and comparability of quantitative results depend on the accuracy of
235 measurements under strictly-defined conditions. A conceptually clearly-defined framework is
236 also required to warrant meaningful interpretation and comparability of experimental outcomes
237 carried out by research groups at different institutes. With an emphasis on quality of research,
238 collected data can be useful far beyond the specific question of a specific experiment. Vague or
239 ambiguous jargon can lead to confusion and may relegate valuable signals to wasteful noise.
240 For this reason, measured values must be expressed in standardized units for each parameter
241 used to define mitochondrial respiratory function. Standardization of nomenclature and

242 technical terms is essential to improve the awareness of the intricate meaning of divergent
243 scientific vocabulary. The focus on coupling states, the protonmotive force and fluxes through
244 metabolic pathways of aerobic energy transformation in mitochondrial preparations is a first
245 step in the attempt to generate a harmonized and conceptually oriented nomenclature in
246 bioenergetics and mitochondrial physiology. Coupling states of intact cells and respiratory
247 control by fuel substrates and specific inhibitors of respiratory enzymes will be reviewed in
248 subsequent communications.

249

250 **2. Respiratory coupling states in mitochondrial preparations**

251 *‘Every professional group develops its own technical jargon for talking about*
252 *matters of critical concern ... People who know a word can share that idea with*
253 *other members of their group, and a shared vocabulary is part of the glue that holds*
254 *people together and allows them to create a shared culture’ (Miller 1991).*

255

256 **Mitochondrial preparations** are defined as either isolated mitochondria, or tissue and
257 cellular preparations in which the barrier function of the plasma membrane is disrupted. The
258 plasma membrane separates the cytosol, nucleus and organelles (the intracellular compartment)
259 from the environment of the cell. The plasma membrane consists of a lipid bilayer, embedded
260 proteins and attached organic molecules which collectively control the selective permeability
261 of ions, organic molecules and particles across the cell boundary. The intact plasma membrane,
262 therefore, prevents the passage of many water-soluble mitochondrial substrates, such as
263 succinate or ADP, that are required for the analysis of respiratory capacity at kinetically
264 saturating concentrations, thus limiting the scope of investigations into mitochondrial
265 respiratory function in intact cells. The cholesterol content of the plasma membrane is high
266 compared to mitochondrial membranes. Therefore, mild detergents, such as digitonin and
267 saponin, can be applied to selectively permeabilize the plasma membrane by interaction with

268 cholesterol and allow free exchange of cytosolic components with ions and organic molecules
269 of the immediate cell environment, while maintaining the integrity and localization of
270 organelles, cytoskeleton and the nucleus. Application of optimum concentrations of these mild
271 detergents leads to the complete loss of cell viability, tested by nuclear staining, while
272 mitochondrial function remains unaffected, as shown by an unaltered respiration rate of
273 mitochondria after the addition of such low concentrations of digitonin and saponin. In addition
274 to mechanical permeabilization during homogenization of fresh tissue, saponin may be applied
275 additionally, to ensure permeabilization of all cells. Crude homogenate and cells permeabilized
276 in the respiration chamber contain all components of the cell at highly diluted concentrations.
277 All mitochondria are retained in chemically permeabilized mitochondrial preparations and
278 crude tissue homogenates. In the preparation of isolated mitochondria, the cells or tissues are
279 homogenized, and the mitochondria are separated from other cell fractions and purified by
280 centrifugation, entailing the loss of a significant fraction of mitochondria. The term
281 mitochondrial preparation does not include further fractionation of mitochondrial components,
282 as well as submitochondrial particles.

283

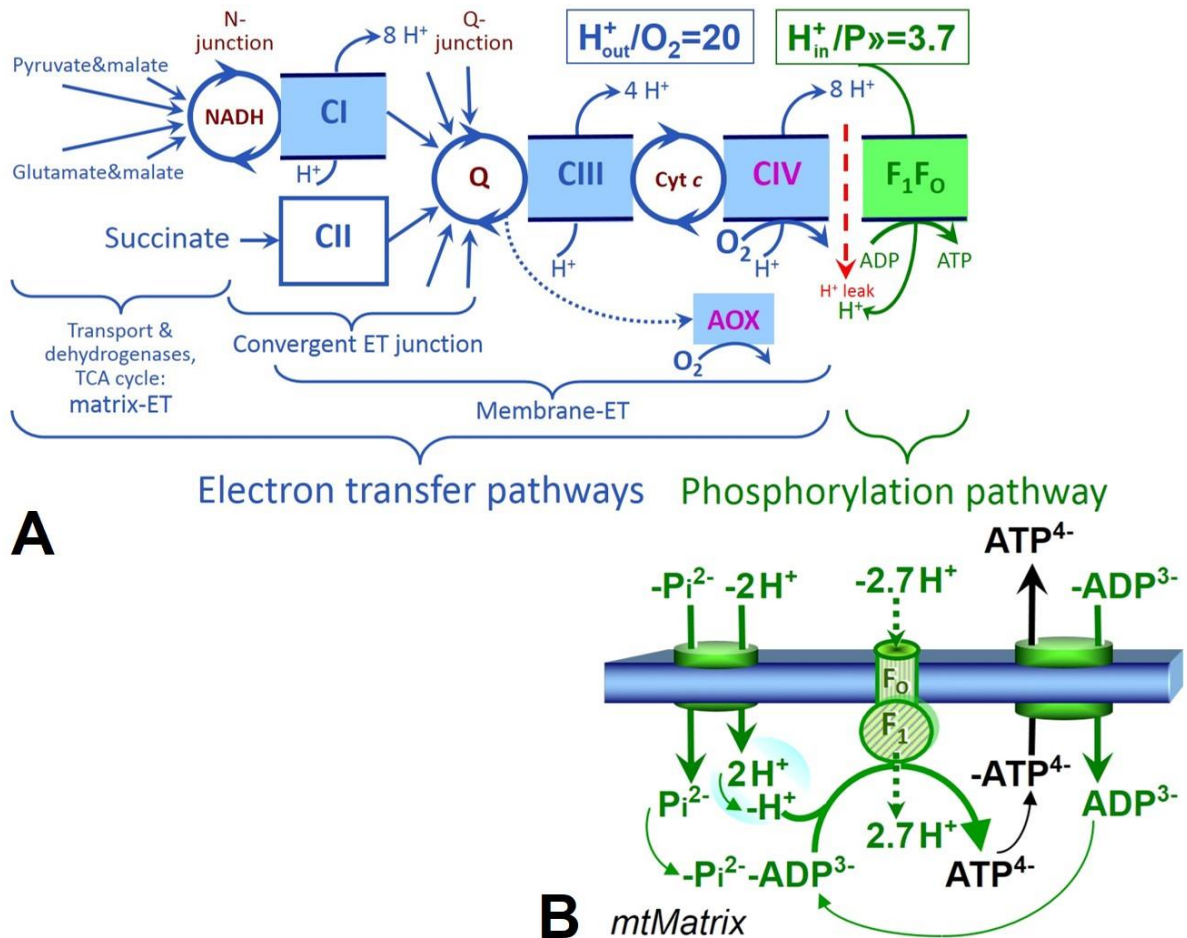
284 *2.1. Three coupling states of mitochondrial preparations and residual oxygen consumption*

285 **Coupling control states:** To extend the classical nomenclature on mitochondrial
286 coupling states (Section 2.4) by a concept-driven terminology that incorporates explicit
287 information on the nature of the respiratory states, the terminology must be general and not
288 restricted to any particular experimental protocol or mitochondrial preparation (Gnaiger 2009).
289 We focus primarily on the conceptual ‘why’, along with clarification of the experimental ‘how’.
290 In the following section, the concept-driven terminology is explained and coupling states are
291 defined. To provide a diagnostic reference for respiratory capacities of core energy metabolism,
292 the capacity of *oxidative phosphorylation*, OXPHOS, is measured at kinetically saturating
293 concentrations of ADP and inorganic phosphate, P_i . The *oxidative* capacity of the electron

294 transfer pathway, ET pathway, reveals the limitation of OXPHOS capacity mediated by the
295 *phosphorylation* pathway. The ET and phosphorylation pathways comprise coupled segments
296 of the OXPHOS pathway. ET capacity is measured as noncoupled respiration by application of
297 *external uncouplers*. The contribution of *intrinsically uncoupled* oxygen consumption is most
298 easily studied by not stimulating or arresting phosphorylation, when oxygen consumption
299 compensates mainly for the proton leak; the corresponding states are collectively classified as
300 LEAK states (**Table 1**). Fuel substrates and ET inhibitors are kept constant, *i.e.* maintaining a
301 defined ET-pathway state, while (1) adding ADP or P_i, (2) inhibiting the phosphorylation
302 pathway, and (3) performing uncoupler titrations to induce different coupling states (**Fig. 1**).

303 **Respiratory capacities and kinetic control:** Coupling control states are established in
304 the study of mitochondrial preparations to obtain reference values for various output variables.
305 Physiological conditions *in vivo* may deviate substantially from these experimentally obtained
306 states. Since kinetically saturating concentrations, *e.g.* of ADP or oxygen, may not apply to
307 physiological intracellular conditions, relevant information is obtained in studies of kinetic
308 responses to conditions intermediate between the LEAK state at zero [ADP] and the OXPHOS
309 state at saturating [ADP], or of respiratory capacities in the range between kinetically saturating
310 [O₂] and anoxia (Gnaiger 2001). We define respiratory capacities, comparable to channel
311 capacity in information theory, as the upper bound of the rate of respiration measured in defined
312 coupling and pathway control states of mitochondrial preparations.

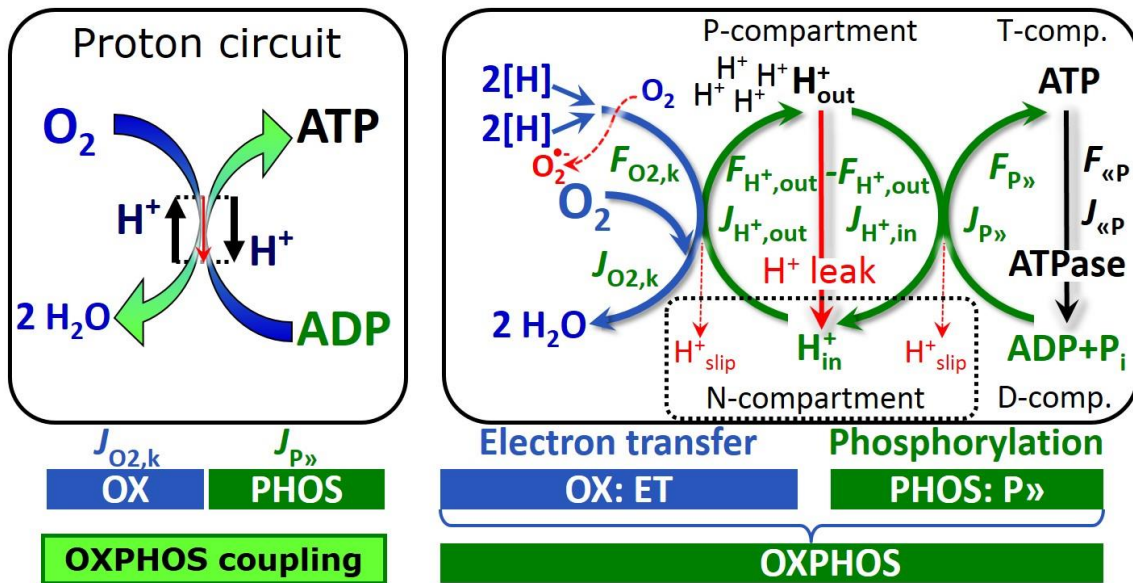
313



314

315 **Fig. 1. The oxidative phosphorylation pathway, OXPHOS pathway. (A)** Electron transfer, ET,
 316 coupled to phosphorylation. Multiple convergent electron transfer pathways are shown from NADH and
 317 succinate; additional arrows indicate electron entry through electron transferring flavoprotein,
 318 glycerophosphate dehydrogenase, dihydro-orotate dehydrogenase, choline dehydrogenase, and
 319 sulfide-ubiquinone oxidoreductase. The branched pathway of oxygen consumption by alternative quinol
 320 oxidase (AOX) is indicated by the dotted arrow. H^+_{out}/O_2 is the ratio of outward proton flux from the matrix
 321 space to catabolic O_2 flux in the NADH-linked pathway. $H^+_{in}/P \gg$ is the ratio of inward proton flux from the
 322 inter-membrane space to the flux of phosphorylation of ADP to ATP. Due to proton leak and slip these
 323 are not fixed stoichiometries. **(B)** Phosphorylation pathway catalyzed by the F₁F₀ ATP synthase,
 324 adenine nucleotide translocase, and inorganic phosphate transporter. The $H^+_{in}/P \gg$ stoichiometry is the
 325 sum of the coupling stoichiometry in the ATP synthase reaction ($-2.7 H^+$ from the intermembrane space,
 326 $2.7 H^+$ to the matrix) and the proton balance in the translocation of ADP²⁻, ATP³⁻ and Pi²⁻. See Eqs. 3
 327 and 4 for further explanation. Modified from (A) Lemieux *et al.* (2017) and (B) Gnaiger (2014).

328



329

330 **Fig. 2. The proton circuit and coupling in oxidative phosphorylation (OXPHOS).** Oxygen flux, $J_{O_2,k}$,331 through the catabolic electron transfer (ET) pathway k is coupled to flux through the phosphorylation332 pathway of ADP to ATP , $J_{P\gg}$, by the proton pumps of the ET pathway, pushing the outward proton flux,333 $J_{H^+,out}$, and generating the output protonmotive force, $F_{H^+,out}$. ATP synthase is coupled to inward proton334 flux, $J_{H^+,in}$, to phosphorylate ADP with inorganic phosphate to ATP , driven by the input protonmotive335 force, $F_{H^+,in} = -F_{H^+,out}$. $2[H]$ indicates the reduced hydrogen equivalents of fuel substrates that provide the336 chemical input force, $F_{O_2,k}$ [kJ/mol O_2], of the catabolic reaction k with oxygen (Gibbs energy of reaction337 per mole O_2 consumed in reaction k), typically in the range of -460 to -480 kJ/mol. The output force is338 given by the phosphorylation potential difference (ADP phosphorylated to ATP), $F_{P\gg}$, which varies *in vivo*339 ranging from about 48 to 62 kJ/mol under physiological conditions. Fluxes, J_B , and forces, F_B , are340 expressed in either chemical units, [mol·s⁻¹·m⁻³] and [J·mol⁻¹] respectively, or electrical units, [C·s⁻¹·m⁻³]341 and [J·C⁻¹] respectively, per volume, V [m³], of the system. The system defined by the boundaries shown

342 as a full black line is not a black box, but is analysed as a compartmental system. The negative

343 compartment (N-compartment, enclosed by the dotted line) is the matrix space, separated from the

344 positive compartment (P-compartment) by the inner mitochondrial membrane. $ADP+P_i$ and ATP are the

345 substrate- and product-compartments (scalar D- and T-comp.), respectively. Chemical potentials of all

346 substrates and products involved in the scalar reactions are measured in the P-compartment for

347 calculation of the scalar forces $F_{O_2,k}$ and $F_{P\gg} = -F_{\ll P}$ (**Box 2**). Modified from Gnaiger (2014).

348

349 **Phosphorylation, P»:** *Phosphorylation* in the context of OXPHOS is defined as
350 phosphorylation of ADP to ATP. On the other hand, the term phosphorylation is used generally
351 in many different contexts, *e.g.* protein phosphorylation. This justifies consideration of a
352 symbol more discriminating and specific than P as used in the P/O ratio (phosphate to atomic
353 oxygen ratio), where P indicates phosphorylation of ADP to ATP or GDP to GTP. We propose
354 the symbol P» for the endergonic direction of phosphorylation ADP→ATP, and likewise the
355 symbol «P for the corresponding exergonic hydrolysis ATP→ADP (**Fig. 2; Box 3**). ATP
356 synthase is the proton pump of the phosphorylation pathway (**Fig. 1B**). P» may also involve
357 substrate-level phosphorylation as part of the tricarboxylic acid cycle (succinyl-CoA ligase)
358 and phosphorylation of ADP catalyzed by phosphoenolpyruvate carboxykinase, adenylate
359 kinase, creatine kinase, hexokinase and nucleoside diphosphate kinase (NDPK). Kinase cycles
360 are involved in intracellular energy transfer and signal transduction for regulation of energy
361 flux. In isolated mammalian mitochondria ATP production catalyzed by adenylate kinase,
362 $2\text{ADP} \leftrightarrow \text{ATP} + \text{AMP}$, proceeds without fuel substrates in the presence of ADP (Komlódi and
363 Tretter 2017). $J_{\text{P»}}/J_{\text{O}_2, \text{k}}$ (P»/O₂) is two times the ‘P/O’ ratio of classical bioenergetics. The
364 effective P»/O₂ ratio is diminished by: (1) the proton leak across the inner mitochondrial
365 membrane from low pH in the P-phase to high pH in the N-phase (P, positive; N, negative); (2)
366 cycling of other cations; (3) proton slip in the proton pumps when a proton effectively is not
367 pumped; and (4) electron leak in the univalent reduction of oxygen (O₂; dioxygen) to superoxide
368 anion radical (O₂^{•-}).

369

370

371

372

373

374

375 **Table 1. Coupling states and residual oxygen consumption in mitochondrial**
 376 **preparations in relation to respiration and phosphorylation rate, $J_{O_2,k}$ and $J_{P_{\gg}}$,**
 377 **and protonmotive force, $F_{H^+,out}$.** Coupling states are established at kinetically
 378 saturating concentrations of fuel substrates and O_2 .

State	$J_{O_2,k}$	$J_{P_{\gg}}$	$F_{H^+,out}$	Inducing factors	Limiting factors
LEAK	L ; low proton leak-dependent respiration	0	max.	Proton leak, slip, and cation cycling	$J_{P_{\gg}}=0$: (1) without ADP, L_N ; (2) max. ATP/ADP ratio, L_T ; or (3) inhibition of the phosphorylation pathway, L_{Omy}
OXPHOS	P ; high ADP-stimulated respiration	max.	high	Kinetically saturating [ADP] and $[P_i]$	$J_{P_{\gg}}$ by phosphorylation pathway; or $J_{O_2,k}$ by ET pathway capacity
ET	E ; max. noncoupled respiration	0	low	Optimal external uncoupler concentration for max. oxygen flux	$J_{O_2,k}$ by ET pathway capacity
ROX	R_{ox} ; min. residual O_2 consumption	0	0	$J_{O_2,Rox}$ in non-ET pathway oxidation reactions	Full inhibition of ET pathway or absence of fuel substrates

379
 380
 381 **LEAK state (Fig. 3):** The
 382 LEAK state is defined as a state
 383 of mitochondrial respiration
 384 when O_2 flux mainly
 385 compensates for the proton leak
 386 in the absence of ATP synthesis,
 387 at kinetically saturating
 388 concentrations of O_2 and
 389 respiratory substrates. LEAK
 390 respiration is measured to obtain
 391 an indirect estimate of *intrinsic uncoupling* without addition of any experimental uncoupler: (1)

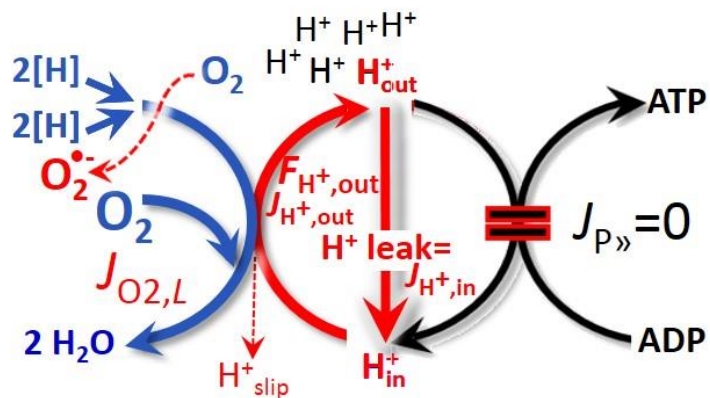


Fig. 3. LEAK state: Phosphorylation is arrested, $J_{P_{\gg}}=0$, and oxygen flux, $J_{O_2,L}$, is controlled mainly by the proton leak, which equals $J_{H^+,in}$, at maximum protonmotive force, $F_{H^+,out}$ (See also Fig. 2).

392 in the absence of adenylates; (2) after depletion of ADP at maximum ATP/ADP ratio; or (3)
393 after inhibition of the phosphorylation pathway by inhibitors of ATP synthase, such as
394 oligomycin, or adenine nucleotide translocase, such as carboxyatractyloside.

395 **Proton leak:** Proton leak is the *uncoupled* process in which protons are translocated
396 across the inner mitochondrial membrane in the dissipative direction of the downhill
397 protonmotive force without coupling to phosphorylation (**Fig. 3**). The proton leak flux depends
398 on the protonmotive force, is a property of the inner mitochondrial membrane, may be enhanced
399 due to possible contaminations by free fatty acids, and is physiologically controlled. In
400 particular, inducible uncoupling mediated by uncoupling protein 1 (UCP1) is physiologically
401 controlled, *e.g.*, in brown adipose tissue. UCP1 is a proton channel of the inner mitochondrial
402 membrane facilitating the conductance of protons across the inner mitochondrial membrane.
403 As consequence of this effective short-circuit, the protonmotive force diminishes, resulting in
404 stimulation of electron transfer to oxygen and heat dissipation without phosphorylation of ADP.
405 Mitochondrial injuries may lead to *dyscoupling* as a pathological or toxicological cause of
406 *uncoupled* respiration, *e.g.*, as a consequence of opening the permeability transition pore.
407 Dyscoupled respiration is distinguished from the experimentally induced *noncoupled*
408 respiration in the ET state. Under physiological conditions, the proton leak is the dominant
409 contributor to the overall leak current.

410 **Proton slip:** Proton slip is the *decoupled* process in which protons are only partially
411 translocated by a proton pump of the ET pathways and slip back to the original compartment
412 (Dufour *et al.* 1996). Proton slip can also happen in association with the ATP-synthase, in which
413 case the proton slips downhill across the membrane to the matrix without contributing to ATP
414 synthesis. In each case, proton slip is a property of the proton pump and increases with the
415 turnover rate of the pump.

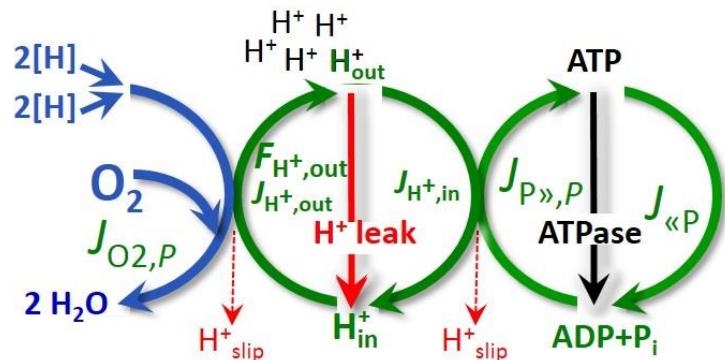
416 **Cation cycling:** Proton leak is a leak current of protons. There can be other cation
417 contributors to leak current including calcium and probably magnesium. Calcium current is

418 balanced by mitochondrial Na/Ca exchange, which is balanced by Na/H exchange or K/H
 419 exchange. This is another effective uncoupling mechanism different from proton leak and slip.

420 Small differences of terms, *e.g.*, uncoupled, noncoupled, are easily overlooked and may
 421 be erroneously perceived as identical. Even with an attempt at rigorous definition, the common
 422 use of such terms may remain vague (Table 2).

423 **OXPHOS state (Fig. 4):**

424 The OXPHOS state is defined as
 425 the respiratory state with
 426 kinetically saturating
 427 concentrations of O₂, respiratory
 428 and phosphorylation substrates,
 429 and absence of exogenous
 430 uncoupler, which provides an
 431 estimate of the maximal capacity
 432 of OXPHOS in any given



433 pathway control state. Respiratory capacities at kinetically saturating substrate concentrations
 434 provide reference values or upper limits of performance, aiming at the generation of data sets
 435 for comparative purposes. Any effects of substrate kinetics are thus separated from reporting
 436 actual mitochondrial capacity for oxidation during coupled respiration, against which
 437 physiological activities can be evaluated.

438 **Fig. 4. OXPHOS state:** Phosphorylation, $J_{P\gg}$, is stimulated
 439 by kinetically saturating [ADP] and inorganic phosphate, $[P_i]$,
 440 and is supported by a high protonmotive force, $F_{H^+,out}$. O_2
 441 flux, $J_{O_2,P}$, is highly coupled at a maximum $P\gg/O_2$ ratio,
 442 $J_{P\gg,P}/J_{O_2,P}$ (See also Fig. 2).

433 pathway control state. Respiratory capacities at kinetically saturating substrate concentrations
 434 provide reference values or upper limits of performance, aiming at the generation of data sets
 435 for comparative purposes. Any effects of substrate kinetics are thus separated from reporting
 436 actual mitochondrial capacity for oxidation during coupled respiration, against which
 437 physiological activities can be evaluated.

438 As discussed previously, 0.2 mM ADP does not fully saturate flux in isolated
 439 mitochondria (Gnaiger 2001; Puchowicz *et al.* 2004); greater ADP concentration is required,
 440 particularly in permeabilized muscle fibres and cardiomyocytes, to overcome limitations by
 441 intracellular diffusion and by the reduced conductance of the outer mitochondrial membrane
 442 (Jepihhina *et al.* 2011, Illaste *et al.* 2012, Simson *et al.* 2016) either through interaction with
 443 tubulin (Rostovtseva *et al.* 2008) or other intracellular structures (Birkedal *et al.* 2014). In

444 permeabilized muscle fibre bundles of high respiratory capacity, the apparent K_m for ADP
 445 increases up to 0.5 mM (Saks *et al.* 1998), indicating that >90% saturation is reached only at
 446 >5 mM ADP. Similar ADP concentrations are also required for accurate determination of
 447 OXPHOS capacity in human clinical cancer samples and permeabilized cells (ref). Whereas 2.5
 448 to 5 mM ADP is sufficient to obtain the actual OXPHOS capacity in many types of
 449 permeabilized cell and tissue preparations, experimental validation is required in each specific
 450 case.

451

452 **Table 2. Distinction of terms related to coupling.**

Term	Respiration	$P \gg O_2$	Note
Fully coupled	$P - L$	Max.	OXPHOS capacity corrected for LEAK respiration (Fig. 6)
Coupled	P	High	Phosphorylating respiration with a variable component of intrinsic LEAK respiration (Fig. 4)
Uncoupled, Decoupled	L	0	Non-phosphorylating respiration without added protonophore (Fig. 3)
Noncoupled	E	0	Non-phosphorylating respiration stimulated to maximum flux at optimum uncoupler concentration (Fig. 5)
Dyscoupled	P	Low	Pathologically increased uncoupling, mitochondrial dysfunction

453

454 **Electron transfer state**

455 (**Fig. 5**): The ET state is defined
 456 as the *noncoupled* state with
 457 kinetically saturating
 458 concentrations of O_2 , respiratory
 459 substrate and optimum
 460 *exogenous* uncoupler
 461 concentration for maximum O_2
 462 flux, as an estimate of oxidative

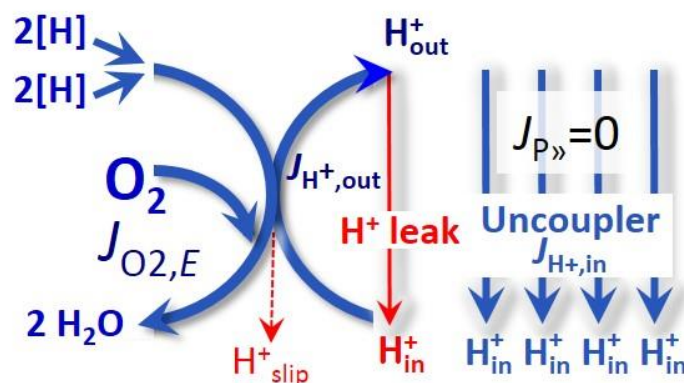


Fig. 5. ET state: Noncoupled respiration, $J_{O_2,E}$ is maximum at optimum exogenous uncoupler concentration and phosphorylation is zero, $J_{P \gg} = 0$ (See also Fig. 2).

463 ET capacity. Inhibition of respiration is observed at higher than optimum uncoupler
464 concentrations. As a consequence of the nearly collapsed protonmotive force, the driving force
465 is insufficient for phosphorylation and $J_{P\gg}=0$.

466 Besides the three fundamental coupling states of mitochondrial preparations, the
467 following respiratory state also is relevant to assess respiratory function:

468 **ROX:** Residual oxygen consumption (ROX) is defined as O₂ consumption due to
469 oxidative side reactions remaining after inhibition of ET. ROX is not a coupling state but
470 represents a baseline that is used to correct mitochondrial respiration in defined coupling states.
471 ROX is not necessarily equivalent to non-mitochondrial respiration, considering oxygen-
472 consuming reactions in mitochondria not related to ET, such as oxygen consumption in
473 reactions catalyzed by monoamine oxidases (type A and B), monooxygenases (cytochrome
474 P450 monooxygenases), dioxygenase (sulfur dioxygenase and trimethyllysine dioxygenase),
475 several hydroxylases, and more. Mitochondrial preparations, especially those obtained from
476 liver, are contaminated by peroxisomes. This fact makes the exact determination of
477 mitochondrial oxygen consumption and mitochondria-associated generation of reactive oxygen
478 species complicated (Schönfeld *et al.* 2009). The dependence of ROX-linked oxygen
479 consumption needs to be studied in detail with respect to non-ET enzyme activities, availability
480 of specific substrates, oxygen concentration, and electron leakage leading to the formation of
481 reactive oxygen species.

482

483 2.2. Coupling states and respiratory rates

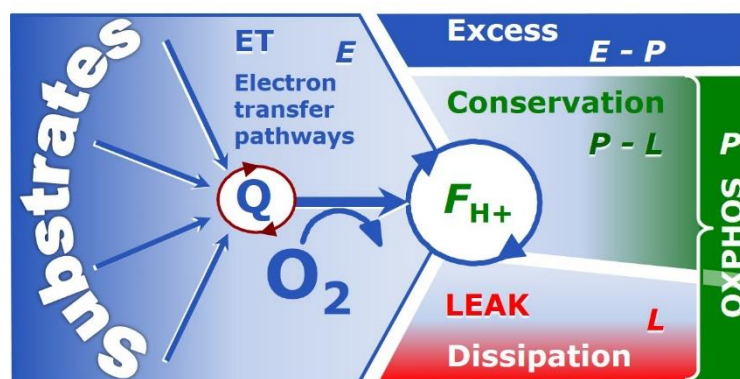
484 It is important to distinguish metabolic pathways from metabolic states and the
485 corresponding metabolic rates; for example: electron transfer pathways (**Fig. 6**), ET state (**Fig.**
486 **5**), and ET capacity, E , respectively (**Table 1**). The protonmotive force is *high* in the OXPHOS
487 state when it drives phosphorylation, *maximum* in the LEAK state of coupled mitochondria,

488 driven by LEAK respiration at a minimum back flux of protons to the matrix side, and *very low*
 489 in the ET state when uncouplers short-circuit the proton cycle (**Table 1**).

490

491 **Fig. 6. Four-compartment model**
 492 **of oxidative phosphorylation.**

493 Respiratory states (ET, OXPHOS,
 494 LEAK) and corresponding rates (E ,
 495 P , L) are connected by the
 496 protonmotive force, $F_{H+,out}$. Electron
 497 transfer capacity, E , is partitioned



498 into (1) dissipative LEAK respiration, L , when the capacity to perform work is irreversibly lost, (2) net
 499 OXPHOS capacity, $P-L$, with partial conservation of the capacity to perform work, and (3) the excess
 500 capacity, $E-P$. Modified from Gnaiger (2014).

501

502 The three coupling states, ET, LEAK and OXPHOS, are presented in a schematic context
 503 with the corresponding respiratory rates, abbreviated as E , L and P , respectively (**Fig. 6**). This
 504 clarifies that E may exceed or be equal to P , but E cannot theoretically be lower than P . $E < P$
 505 must be discounted as an artefact, which may be caused experimentally by: (1) loss of oxidative
 506 capacity during the time course of the respirometric assay, since E is measured subsequently to
 507 P ; (2) using too low uncoupler concentrations; (3) using high uncoupler concentrations which
 508 inhibit ET (Gnaiger 2008); (4) high oligomycin concentrations applied for measurement of L
 509 before titrations of uncoupler, when oligomycin exerts an inhibitory effect on E . On the other
 510 hand, the excess ET capacity is overestimated if non-saturating $[P_i]$ or $[ADP]$ (State 3) are used.

511 $E > P$ is observed in many types of mitochondria, varying between species, tissues and cell
 512 types. It is the excess ET capacity pushing the phosphorylation pathway flux (**Fig. 1B**) to the
 513 limit of its *capacity of utilizing* the protonmotive force. Within any type of mitochondria, the
 514 magnitude of $E > P$ depends on (1) the pathway control state with single or multiple electron
 515 input into the Q-junction and involvement of three or fewer coupling sites determining the

516 H^+_{out}/O_2 coupling stoichiometry (**Fig. 1A**); and (2) the *biochemical coupling efficiency*
517 expressed as $(E-L)/E$, since an increase of L causes P to increase towards the limit of E . The
518 *excess E-P capacity*, $E-P$, therefore, provides a sensitive diagnostic indicator of specific injuries
519 of the phosphorylation pathway, under conditions when E remains constant but P declines
520 relative to controls (**Fig. 6**). Substrate cocktails supporting simultaneous convergent electron
521 transfer to the Q-junction for reconstitution of tricarboxylic acid cycle (TCA cycle) function
522 establish pathway control states with high ET capacity, and consequently increase the
523 sensitivity of the $E-P$ assay.

524 When subtracting L from P , the dissipative LEAK component in the OXPHOS state may
525 be overestimated. This can be avoided by measuring LEAK respiration in a state when the
526 protonmotive force is adjusted to its slightly lower value in the OXPHOS state, *e.g.*, by titration
527 of an ET inhibitor. Any turnover-dependent components of proton leak and slip, however, are
528 underestimated under these conditions (Garlid *et al.* 1993). In general, it is inappropriate to use
529 the term *ATP production* or *ATP turnover* for the difference of oxygen consumption measured
530 in states P and L . The difference $P-L$ is the upper limit of the part of OXPHOS capacity that is
531 freely available for ATP production (corrected for LEAK respiration) and is fully coupled to
532 phosphorylation with a maximum mechanistic stoichiometry (**Fig. 6**).

533

534 2.3. Classical terminology for isolated mitochondria

535 ‘When a code is familiar enough, it ceases appearing like a code; one forgets that
536 there is a decoding mechanism. The message is identical with its meaning’
537 (Hofstadter 1979).

538 Chance and Williams (1955; 1956) introduced five classical states of mitochondrial respiration
539 and cytochrome redox states. **Table 3** shows a protocol with isolated mitochondria in a closed
540 respirometric chamber, defining a sequence of respiratory states.

541
542
543**Table 3. Metabolic states of mitochondria (Chance and Williams, 1956; Table V).**

State	[O ₂]	ADP level	Substrate level	Respiration rate	Rate-limiting substance
1	>0	low	Low	Slow	ADP
2	>0	high	~0	Slow	Substrate
3	>0	high	High	Fast	respiratory chain
4	>0	low	High	Slow	ADP
5	0	high	High	0	Oxygen

544

545 **State 1** is obtained after addition of isolated mitochondria to air-saturated
546 isoosmotic/isotonic respiration medium containing inorganic phosphate, but no fuel substrates
547 and no adenylates, *i.e.*, AMP, ADP, ATP.

548 **State 2** is induced by addition of a high concentration of ADP (typically 100 to 300 μ M),
549 which stimulates respiration transiently on the basis of endogenous fuel substrates and
550 phosphorylates only a small portion of the added ADP. State 2 is then obtained at a low
551 respiratory activity limited by zero endogenous fuel substrate availability (**Table 3**). If addition
552 of specific inhibitors of respiratory complexes, such as rotenone, does not cause a further
553 decline of oxygen consumption, State 2 is equivalent to residual oxygen consumption (See
554 below). If inhibition is observed, undefined endogenous fuel substrates are a confounding factor
555 of pathway control by externally added substrates and inhibitors. In contrast to the original
556 protocol, an alternative sequence of titration steps is frequently applied, in which the alternative
557 State 2 has an entirely different meaning, when this second state is induced by addition of fuel
558 substrate without ADP (LEAK state; in contrast to State 3 as a ROX state as defined in **Table**
559 **2**), followed by addition of ADP.

560 **State 3** is the state stimulated by addition of fuel substrates while the ADP concentration
561 is still high (**Table 3**) and supports coupled energy transformation through oxidative
562 phosphorylation. 'High ADP' is a concentration of ADP specifically selected to allow the
563 measurement of State 3 to State 4 transitions of isolated mitochondria in a closed respirometric
564 chamber. Repeated ADP titration re-establishes State 3 at 'high ADP'. Starting at oxygen

565 concentrations near air-saturation (ca. 200 μM O_2 at sea level and 37 $^\circ\text{C}$), the total ADP
566 concentration added must be low enough (typically 100 to 300 μM) to allow phosphorylation
567 to ATP at a coupled oxygen consumption that does not lead to oxygen depletion during the
568 transition to State 4. In contrast, kinetically saturating ADP concentrations usually are an order
569 of magnitude higher than 'high ADP', *e.g.* 2.5 mM in isolated mitochondria. The abbreviation
570 State 3u is frequently used in bioenergetics, to indicate the state of respiration after titration of
571 an uncoupler, without sufficient emphasis on the fundamental difference between OXPHOS
572 capacity (*well-coupled* with an *endogenous* uncoupled component) and ET capacity
573 (*noncoupled*).

574 **State 4** is a LEAK state which is obtained only if the mitochondrial preparation is intact
575 and well-coupled. Depletion of ADP by phosphorylation to ATP leads to a decline in oxygen
576 consumption in the transition from State 3 to State 4. Under these conditions, a maximum
577 protonmotive force and high ATP/ADP ratio are maintained, and the $\text{P}_{\gg}/\text{O}_2$ ratio can be
578 calculated. State 4 respiration, L_T (**Table 1**), reflects intrinsic proton leak and intrinsic ATP
579 hydrolysis activity. Oxygen consumption in State 4 is an overestimation of LEAK respiration
580 if the contaminating ATP hydrolysis activity recycles some ATP to ADP, $J_{\ll\text{P}}$, which stimulates
581 respiration coupled to phosphorylation, $J_{\text{P}\gg}>0$. This can be tested by inhibition of the
582 phosphorylation pathway using oligomycin, ensuring that $J_{\text{P}\gg}=0$ (State 4o). Alternatively,
583 sequential ADP titrations re-establish State 3, followed by State 3 to State 4 transitions while
584 sufficient oxygen is available. However, anoxia may be reached before exhaustion of ADP
585 (State 5).

586 **State 5** is the state after exhaustion of oxygen in a closed respirometric chamber.
587 Diffusion of oxygen from the surroundings into the aqueous solution may be a confounding
588 factor preventing complete anoxia (Gnaiger 2001).

589 In **Table 3**, only States 3 and 4 (and ‘State 2’ in the alternative protocol without ADP;
 590 not included in the table) are coupling control states, with the restriction that O₂ flux in State 3
 591 may be limited kinetically by non-saturating ADP concentrations (**Table 1**).

592

593 3. The protonmotive force and proton flux

594 3.1. Electric and chemical partial forces versus electrical and chemical units

595 The protonmotive force across the inner mitochondrial membrane (Mitchell and Moyle
 596 1967) was introduced most beautifully in the *Grey Book 1966* (see Mitchell 2011),

$$597 \quad \Delta p_{\text{H}^+} = \Delta \Psi + \Delta \mu_{\text{H}^+}/F \quad (\text{Eq. 1})$$

598 The protonmotive force consists of two partial forces: (1) The electrical part, $\Delta \Psi$, is the
 599 difference of charge (electric potential difference) and is not specific for H⁺. (2) The chemical
 600 part, $\Delta \mu_{\text{H}^+}$, is the chemical potential difference in H⁺, is proportional to the pH difference, and
 601 incorporates the Faraday constant (**Table 4**).

602

603 **Table 4. Protonmotive force and flux matrix.** Rows: Electrical and chemical
 604 isomorphic format (*e* and *n*). The Faraday constant, *F*, converts protonmotive force
 605 and flux from *isomorphic format e* to *n*. Columns: The protonmotive force is the sum of
 606 *partial isomorphic forces* F_{el} and $F_{\text{H}^+, \text{d}}$. In contrast to force (state), the conjugated flux
 607 (rate) cannot be partitioned.

608

State	Force		electric	+ chem.	Unit	Notes
Protonmotive force, <i>e</i>	Δp_{H^+}	=	$\Delta \Psi$	+ $\Delta \mu_{\text{H}^+}/F$	J·C ⁻¹	1 <i>e</i>
Chemiosmotic potential, <i>n</i>	$\Delta \tilde{\mu}_{\text{H}^+}$	=	$\Delta \Psi \cdot F$	+ $\Delta \mu_{\text{H}^+}$	J·mol ⁻¹	1 <i>n</i>
State	Isomorphic force		$F_{\text{el, out}}$	+ $F_{\text{H}^+, \text{d}}$		
Electric charge, <i>e</i>	$F_{\text{H}^+, \text{out}/e}$	=	$F_{\text{el, out}/e}$	+ $F_{\text{H}^+, \text{out}, \text{d}/e}$	J·C ⁻¹	2 <i>e</i>
Amount of substance, <i>n</i>	$F_{\text{H}^+, \text{out}/n}$	=	$F_{\text{el, out}/n}$	+ $F_{\text{H}^+, \text{out}, \text{d}/n}$	J·mol ⁻¹	2 <i>n</i>
Rate	Isomorphic flux		<i>e</i>	or	<i>n</i>	
Electric charge, <i>e</i>	$J_{\text{H}^+, \text{out}/e}$		$J_{\text{H}^+, \text{out}/e}$		C·s ⁻¹ ·m ⁻³	3 <i>e</i>
Amount of substance, <i>n</i>	$J_{\text{H}^+, \text{out}/n}$			$J_{\text{H}^+, \text{out}/n}$	mol·s ⁻¹ ·m ⁻³	3 <i>n</i>

- 609
- 610 1: The Faraday constant, F , is the product of elementary charge ($e=1.602177 \cdot 10^{-19} \cdot \text{C}$) and the
- 611 Avogadro (Loschmidt) constant ($N_A=6.022136 \cdot 10^{23} \cdot \text{mol}^{-1}$), $F=eN_A=96,485.3 \text{ C/mol}$. $\Delta\tilde{\mu}_{\text{H}^+}$ is the
- 612 chemiosmotic potential difference. $1e$ and $1n$ are the classical representations of $2e$ and $2n$.
- 613 2: The protonmotive force is $F_{\text{H}^+, \text{out}}$, expressed either in isomorphic format e or n . $F_{\text{el}/e} \equiv \Delta\Psi$ is the partial
- 614 protonmotive force (el) acting generally on charged motive molecules (*i.e.* ions that are displaceable
- 615 across the inner mitochondrial membrane). In contrast, $F_{\text{H}^+, \text{d}/n} \equiv \Delta\mu_{\text{H}^+}$ is the partial protonmotive force
- 616 specific for proton displacement (H^+). The sign of the force is negative for exergonic transformations
- 617 in which exergy is lost or dissipated, and positive for endergonic transformations which conserve
- 618 exergy from a coupled exergonic process (**Box 3**).
- 619 3: The sign of the flux depends on the definition of the compartmental direction of the translocation (**Fig.**
- 620 **2**). Flux x force = $J_{\text{H}^+, \text{out}/e} \cdot F_{\text{H}^+, \text{out}/e} = J_{\text{H}^+, \text{out}/n} \cdot F_{\text{H}^+, \text{out}/n} = \text{Volume-specific power} [\text{J} \cdot \text{s}^{-1} \cdot \text{m}^{-3} = \text{W} \cdot \text{m}^{-3}]$.

621

622 **Faraday constant**, $F=eN_A$ [C/mol] (**Table 4**), enables the conversion between

623 protonmotive force, $F_{\text{H}^+, \text{out}/e} \equiv \Delta p_{\text{H}^+}$ [J/C], expressed per *motive charge*, e [C], and protonmotive

624 force or electrochemical potential difference, $F_{\text{H}^+, \text{out}/n} \equiv \Delta\tilde{\mu}_{\text{H}^+} = \Delta p_{\text{H}^+} \cdot F$ [J/mol], expressed per

625 *motive amount of protons*, n [mol]. Proton charge, e , and amount of substance, n , define the

626 units for the isomorphic formats. Taken together, F converts protonmotive force and flux from

627 isomorphic format e to n (Eq. 2; see also **Table 4**, Note 2),

$$628 \quad F_{\text{H}^+, \text{out}/n} = F_{\text{H}^+, \text{out}/e} \cdot eN_A \quad (\text{Eq. 2.1})$$

$$629 \quad J_{\text{H}^+, \text{out}/n} = J_{\text{H}^+, \text{out}/e} / (eN_A) \quad (\text{Eq. 2.2})$$

630 In each format, the protonmotive force is expressed as the sum of two partial forces. The

631 concept expressed by the complex symbols in Eq. 1 can be explained and visualized more easily

632 by *partial isomorphic forces* as the components of the protonmotive force:

633 **Electrical part of the protonmotive force:** (1) Isomorph e : $F_{\text{el}/e} \equiv \Delta\Psi$ is the electrical

634 part of the protonmotive force expressed in units joule per coulomb, *i.e.* volt [$\text{V}=\text{J}/\text{C}$]. $F_{\text{el}/e}$ is

635 defined as partial Gibbs energy change per *motive elementary charge*, e [C], not specific for

636 proton charge (**Table 4**, Note 2e). (2) Isomorph n : $F_{\text{el}/n} \equiv \Delta\Psi \cdot F$ is the electric force expressed

637 in units joule per mole [J/mol], defined as partial Gibbs energy change per *motive amount of*
 638 *charge*, n [mol], not specific for proton charge (**Table 4**, Note 2*n*).

639 **Chemical part of the protonmotive force:** (1) Isomorph n : $F_{d,H+/n} \equiv \Delta\mu_{H^+}$ is the chemical
 640 part (diffusion, displacement of H^+) of the protonmotive force expressed in units joule per mole
 641 [J/mol]. $F_{d,H+/n}$ is defined as partial Gibbs energy change per *motive amount of protons*, n [mol]
 642 (**Table 4**, Note 2*n*). (2) Isomorph e : $F_{d,H+/e} \equiv \Delta\mu_{H^+}/F$ is the chemical force expressed in units
 643 joule per coulomb [V], defined as partial Gibbs energy change per *motive amount of protons*
 644 *expressed in units of electric charge*, e [C], but specific for proton charge (**Table 4**, Note 2*e*).

645 Protonmotive means that there is a potential for the movement of protons, and force is a
 646 measure of the potential for motion. Motion is relative and not absolute (Principle of Galilean
 647 Relativity); likewise there is no absolute potential, but (isomorphic) forces are potential
 648 differences. An electric partial force expressed in the format of electric charge, $F_{el/e}$, of -0.2 V
 649 (**Table 5**, Note 5*e*) is equivalent to force in the format of amount, $F_{el,H+/n}$, of $19 \text{ kJ}\cdot\text{mol}^{-1} H^+_{out}$
 650 (Note 5*n*). For a ΔpH of 1 unit, the chemical partial force in the format of amount, $F_{d,H+/n}$,
 651 changes by $5.9 \text{ kJ}\cdot\text{mol}^{-1}$ (**Table 5**, Note 6*n*) and chemical force in the format of charge $F_{d,H+/e}$
 652 changes by 0.06 V (Note 6*e*). Considering a driving force of $-470 \text{ kJ}\cdot\text{mol}^{-1} O_2$ for oxidation, the
 653 thermodynamic limit of the H^+_{out}/O_2 ratio is reached at a value of $470/19=24$, compared to a
 654 mechanistic stoichiometry of 20 (**Fig. 1**).

655

656 3.2. Definitions

657 **Control and regulation:** The terms metabolic *control* and *regulation* are frequently used
 658 synonymously, but are distinguished in metabolic control analysis: ‘We could understand the
 659 regulation as the mechanism that occurs when a system maintains some variable constant over
 660 time, in spite of fluctuations in external conditions (homeostasis of the internal state). On the
 661 other hand, metabolic control is the power to change the state of the metabolism in response to
 662 an external signal’ (Fell 1997). Respiratory control may be induced by experimental control

663 signals that *exert* an influence on: (1) ATP demand and ADP phosphorylation rate; (2) fuel
664 substrate composition, pathway competition; (3) available amounts of substrates and oxygen,
665 *e.g.*, starvation and hypoxia; (3) the protonmotive force, redox states, flux-force relationships,
666 coupling and efficiency; (4) Ca^{2+} and other ions including H^+ ; (5) inhibitors, *e.g.*, nitric oxide
667 or intermediary metabolites, such as oxaloacetate; (6) signalling pathways and regulatory
668 proteins, *e.g.* insulin resistance, transcription factor HIF-1 or inhibitory factor 1. *Mechanisms*
669 of respiratory control and regulation include adjustments of (1) enzyme activities by allosteric
670 mechanisms and phosphorylation, (2) enzyme content, concentrations of cofactors and
671 conserved moieties (such as adenylates, nicotinamide adenine dinucleotide [NAD^+/NADH],
672 coenzyme Q, cytochrome *c*); (3) metabolic channeling by supercomplexes; and (4)
673 mitochondrial density (enzyme concentrations and membrane area) and morphology (cristae
674 folding, fission and fusion). (5) Mitochondria are targeted directly by hormones, thereby
675 affecting their energy metabolism (Lee *et al.* 2013; Gerö and Szabo 2016; Price and Dai 2016;
676 Moreno *et al.* 2017). Evolutionary or acquired differences in the genetic and epigenetic basis
677 of mitochondrial function (or dysfunction) between subjects and gene therapy; age; gender,
678 biological sex, and hormone concentrations; life style including exercise and nutrition; and
679 environmental issues including thermal, atmospheric, toxicological and pharmacological
680 factors, exert an influence on all control mechanisms listed above (for reviews, see Brown 1992;
681 Gnaiger 1993a, 2009; 2014; Paradies *et al.* 2014; Morrow *et al.* 2017).

682 **Respiratory control and response:** Lack of control by a metabolic pathway, *e.g.*
683 phosphorylation pathway, does mean that there will be no response to a variable activating it,
684 *e.g.* [ADP]. However, the reverse is not true as the absence of a response to [ADP] does not
685 exclude the phosphorylation pathway from having some degree of control. The degree of
686 control of a component of the OXPHOS pathway on an output variable, such as oxygen flux,
687 will in general be different from the degree of control on other outputs, such as phosphorylation
688 flux or proton leak flux (**Box 2**). As such, it is necessary to be specific as to which input and

689 output are under consideration (Fell 1997). Therefore, the term respiratory control is elaborated
690 in more detail in the following section.

691 **Respiratory coupling control:** Respiratory control refers to the ability of mitochondria
692 to adjust oxygen consumption in response to external control signals by engaging various
693 mechanisms of control and regulation. Respiratory control is monitored in a mitochondrial
694 preparation under conditions defined as respiratory states. When phosphorylation of ADP to
695 ATP is stimulated or depressed, an increase or decrease is observed in electron flux linked to
696 oxygen consumption in respiratory coupling states of intact mitochondria ('controlled states' in
697 the classical terminology of bioenergetics). Alternatively, coupling of electron transfer with
698 phosphorylation is disengaged by disruption of the integrity of the inner mitochondrial
699 membrane or by uncouplers, functioning like a clutch in a mechanical system. The
700 corresponding coupling control state is characterized by high levels of oxygen consumption
701 without control by phosphorylation ('uncontrolled state'). Energetic coupling is defined in **Box**
702 **4**. Loss of coupling by intrinsic uncoupling and decoupling, or pathological dyscoupling lowers
703 the efficiency. Such generalized uncoupling is different from switching to mitochondrial
704 pathways that involve fewer than three proton pumps ('coupling sites': Complexes CI, CIII and
705 CIV), bypassing CI through multiple electron entries into the Q-junction (**Fig. 1**). A bypass of
706 CIII and CIV is provided by alternative oxidases, which reduce oxygen without proton
707 translocation. Reprogramming of mitochondrial pathways may be considered as a switch of
708 gears (changing the stoichiometry) rather than uncoupling (loosening the stoichiometry).

709 **Pathway control states** are obtained in mitochondrial preparations by depletion of
710 endogenous substrates and addition to the mitochondrial respiration medium of fuel substrates
711 (CHNO) and specific inhibitors, activating selected mitochondrial pathways (**Fig. 1**). Coupling
712 control states and pathway control states are complementary, since mitochondrial preparations
713 depend on an exogenous supply of pathway-specific fuel substrates and oxygen (Gnaiger 2014).

714

715

 716 **Box 2: Metabolic fluxes and flows: vectorial and scalar**

717 In mitochondrial electron transfer (**Fig. 1**), vectorial transmembrane proton flux is coupled
 718 through the proton pumps CI, CIII and CIV to the catabolic flux of scalar reactions, collectively
 719 measured as oxygen flux. In **Fig. 2**, the scalar catabolic reaction, k , of oxygen consumption,
 720 $J_{O_2,k}$ [$\text{mol}\cdot\text{s}^{-1}\cdot\text{m}^{-3}$], is expressed as oxygen flux per volume, V [m^3], of the instrumental chamber
 721 (the system).

722 Fluxes are *vectors*, if they have *spatial* direction in addition to magnitude. A vector flux
 723 (surface-density of flow) is expressed per unit cross-sectional area, A [m^2], perpendicular to the
 724 direction of flux. If *flows*, I , are defined as extensive quantities of the *system*, as vector or scalar
 725 flow, I or I [$\text{mol}\cdot\text{s}^{-1}$], respectively, then the corresponding vector and scalar *fluxes*, J , are
 726 obtained as $J=I\cdot A^{-1}$ [$\text{mol}\cdot\text{s}^{-1}\cdot\text{m}^{-2}$] and $J=I\cdot V^{-1}$ [$\text{mol}\cdot\text{s}^{-1}\cdot\text{m}^{-3}$], respectively, expressing flux as an
 727 area-specific vector or volume-specific scalar quantity.

728 Vectorial transmembrane proton flux, $J_{H^+,out}$, is analyzed in a heterogenous
 729 compartmental system as a quantity with *directional* but not *spatial* information. Translocation
 730 of protons across the inner mitochondrial membrane has a defined direction, either from the
 731 negative compartment (matrix space; N-phase) to the positive compartment (inter-membrane
 732 space; P-phase) or *vice versa* (**Fig. 2**). The arrows defining the direction of the translocation
 733 between the two compartments may point upwards or downwards, right or left, without any
 734 implication that these are actual directions in space. The ‘upper’ compartment of the P-phase is
 735 neither above nor below the N-phase in a spatial sense, but can be visualized arbitrarily in a
 736 figure as the upper compartment (**Fig. 2**). In general, the *compartmental direction* of vectorial
 737 translocation from the N-phase to the P-phase is defined by assigning the initial and final state
 738 as *ergodynamic compartments*, $H^+_{in} \rightarrow H^+_{out}$, respectively, related to work (erg = work) that
 739 must be performed to lift the proton from a lower to a higher electrochemical potential or from
 740 the lower to the higher ergodynamic compartment (Gnaiger 1993b).

741 In direct analogy to *vectorial* translocation, the direction of a *scalar* chemical reaction, A
 742 \rightarrow B, is defined by assigning substrates and products, A and B, as ergodynamic compartments.
 743 O_2 is defined as a substrate in respiratory O_2 consumption, which together with the fuel
 744 substrates comprises the substrate compartment of the catabolic reaction (**Fig. 2**). Volume-
 745 specific scalar O_2 flux is coupled (**Box 4**) to vectorial translocation. In order to establish a
 746 quantitative relation between the coupled fluxes, both $J_{\text{O}_2, \text{k}}$ and $J_{\text{H}^+, \text{out}}$ must be expressed in
 747 identical units ($[\text{mol}\cdot\text{s}^{-1}\cdot\text{m}^{-3}]$ or $[\text{C}\cdot\text{s}^{-1}\cdot\text{m}^{-3}]$), yielding the $\text{H}^+_{\text{out}}/\text{O}_2$ ratio (**Fig. 1**). The *vectorial*
 748 proton flux in compartmental translocation has *compartmental direction*, distinguished from a
 749 *vector* flux with *spatial direction*. Likewise, the corresponding protonmotive force is defined
 750 as an electrochemical potential *difference* between two compartments, in contrast to a *gradient*
 751 across the membrane or a vector force with defined spatial direction.

752

753 **The steady-state:** Mitochondria represent a thermodynamically open system functioning
 754 as a biochemical transformation system in non-equilibrium states. State variables (protonmotive
 755 force; redox states) and metabolic fluxes (*rates*) are measured in defined mitochondrial
 756 respiratory *states*. Strictly, steady states can be obtained only in open systems, in which changes
 757 due to *internal* transformations, *e.g.*, O_2 consumption, are instantaneously compensated for by
 758 *external* fluxes *e.g.*, O_2 supply, such that oxygen concentration does not change in the system
 759 (Gnaiger 1993b). Mitochondrial respiratory states monitored in closed systems satisfy the
 760 criteria of pseudo-steady states for limited periods of time, when changes in the system
 761 (concentrations of O_2 , fuel substrates, ADP, P_i , H^+) do not exert significant effects on metabolic
 762 fluxes (respiration, phosphorylation). Such pseudo-steady states require respiratory media with
 763 sufficient buffering capacity and kinetically saturating concentrations of substrates to be
 764 maintained, and thus depend on the kinetics of the processes under investigation. Proton
 765 turnover, $J_{\infty \text{H}^+}$, and ATP turnover, $J_{\infty \text{P}}$, proceed in the steady-state at constant $F_{\text{H}^+, \text{out}}$, when $J_{\infty \text{H}^+}$
 766 $= J_{\text{H}^+, \text{out}} = J_{\text{H}^+, \text{in}}$, and at constant $F_{\text{P}, \gg}$, when $J_{\infty \text{P}} = J_{\text{P}, \gg} = J_{\ll \text{P}}$ (**Fig. 2**).

767

768 Box 3: Endergonic and exergonic transformations, exergy and dissipation

769 A chemical reaction, or any transformation, is exergonic if the Gibbs energy change (exergy)
770 of the reaction is negative at constant temperature and pressure. The sum of Gibbs energy
771 changes of all internal transformations in a system can only be negative, *i.e.* exergy is
772 irreversibly dissipated. Endergonic reactions are characterized by positive Gibbs energies of
773 reaction and cannot proceed spontaneously in the forward direction as defined. For instance,
774 the endergonic reaction $P \rightarrow$ is coupled to exergonic catabolic reactions, such that the total Gibbs
775 energy change is negative, *i.e.* exergy must be dissipated for the reaction to proceed (**Fig. 2**).

776 In contrast, energy cannot be lost or produced in any internal process, which is the key
777 message of the first law of thermodynamics. Thus mitochondria are the sites of energy
778 transformation but not energy production. Open and closed systems can gain energy and exergy
779 only by external fluxes, *i.e.* uptake from the environment. Exergy is the potential to perform
780 work. In the framework of flux-force relationships (**Box 4**), the *partial* derivative of Gibbs
781 energy per advancement of a transformation is an isomorphic force, F_{tr} (**Table 5**, Note 2). In
782 other words, force is equal to exergy/motive unit (in integral form, this definition takes care of
783 non-isothermal processes). This formal generalization represents an appreciation of the
784 conceptual beauty of Peter Mitchell's innovation of the protonmotive force against the
785 background of the established paradigm of the electromotive force (emf) defined at the limit of
786 zero current (Cohen *et al.* 2008).

787

788

789

790

791

792

793 **Table 5. Power, exergy, force, flux, and advancement.**
794

Expression	Symbol	Definition	Unit	Notes
Power, volume-specific	$P_{V,tr}$	$P_{V,tr} = J_{tr} \cdot F_{tr} = \partial_{tr}G \cdot \partial t^{-1}$	$W = J \cdot s^{-1} \cdot m^{-3}$	1
Force, isomorphic	F_{tr}	$F_{tr} = \partial_{tr}G \cdot \partial_{tr}\xi^{-1}$	$J \cdot x^{-1}$	2
Flux, isomorphic	J_{tr}	$J_{tr} = d_{tr}\xi \cdot dt^{-1} \cdot V^{-1}$	$x \cdot s^{-1} \cdot m^{-3}$	3
Advancement, n	$d_{tr}\xi_{H+/n}$	$d_{tr}\xi_{H+/n} = d_{tr}n_{H+} \cdot v_{H+}^{-1}$	Mol	$4n$
Advancement, e	$d_{tr}\xi_{H+/e}$	$d_{tr}\xi_{H+/e} = d_{tr}e_{H+} \cdot v_{H+}^{-1}$	C	$4e$
Electric partial force, e	$F_{el/e}$	$F_{el/e} \equiv \Delta\Psi$	V	$5e$
Electric partial force, n	$F_{el/n}$	$\Delta\Psi \cdot F = 96.5 \cdot \Delta\Psi$	$kJ \cdot mol^{-1}$	$5n$
Chemical partial force, e	$F_{d,H+/e}$	$\Delta\mu_{H+}/F = -$ $\ln(10) \cdot RT/F \cdot \Delta pH$ at 37 °C $= -0.06 \cdot \Delta pH$	V $J \cdot C^{-1}$	$6e$
Chemical partial force, n	$F_{d,H+/n}$	$\Delta\mu_{H+} = -\ln(10) \cdot RT \cdot \Delta pH$ at 37 °C $= -5.9 \cdot \Delta pH$	$J \cdot mol^{-1}$ $kJ \cdot mol^{-1}$	$6n$

795
796 1 to 4: An isomorphic motive entity or transformant, expressed in units x , is defined for any
797 transformation, tr. $x = \text{mol}$ or C in proton translocation.

798 2: $\partial_{tr}G$ [J] is the partial Gibbs energy change in the advancement of transformation tr.

799 3: For $x = \text{C}$, flow is electric current, I_{el} [$A = C \cdot s^{-1}$], vector flux is electric current density per area, J_{el} ,
800 and compartmental flux is electric current density per volume, I_{el} [$A \cdot m^{-3}$].

801 $4n$: For a chemical reaction, the advancement of reaction r is $d_r\xi_B = d_r n_B \cdot v_B^{-1}$ [mol]. The stoichiometric
802 number is $v_B = -1$ or $v_B = 1$, depending on B being a product or substrate, respectively, in reaction r
803 involving one mole of B. The conjugated *intensive* molar quantity, $F_{B,r} = \partial_r G / \partial_r \xi_B$ [$J \cdot mol^{-1}$], is the
804 chemical force of reaction or *reaction-motive* force per stoichiometric amount of B. In reaction
805 kinetics, $d_r n_B$ is expressed as a volume-specific quantity, which is the partial contribution to the
806 total concentration change of B, $d_r c_B = d_r n_B / V$ and $d c_B = d n_B / V$, respectively. In open systems with
807 constant volume V , $d c_B = d_r c_B + d_e c_B$, where r indicates the *internal* reaction and e indicates the
808 *external* flux of B into the unit volume of the system. At steady state the concentration does not
809 change, $d c_B = 0$, when $d_r c_B$ is compensated for by the external flux of B, $d_r c_B = -d_e c_B$ (Gnaiger
810 1993b). Alternatively, $d c_B = 0$ when B is held constant by different coupled reactions in which B
811 acts as a substrate or a product.

812 4e: Scalar potential difference across the mitochondrial membrane. In a scalar electric transformation
 813 (flux of charge, *i.e.* volume-specific current, from the matrix space to the intermembrane and
 814 extramitochondrial space) the motive force is the difference of charge (**Box 2**). The endergonic
 815 direction of translocation is defined in **Fig. 2** as $H^+_{in} \rightarrow H^+_{out}$.

816 5n: $F=96.5 \text{ (kJ}\cdot\text{mol}^{-1})/\text{V}$.

817 6: The electric partial force is independent of temperature (Note 5), but the chemical partial force
 818 depends on absolute temperature, T [K].

819 6e: RT is the gas constant times absolute temperature. $\ln(10)\cdot RT/F = 59.16$ and 61.54 mV at 298.15
 820 and 310.15 K (25 and 37 °C), respectively.

821 6n: $\ln(10)\cdot RT = 5.708$ and $5.938 \text{ kJ}\cdot\text{mol}^{-1}$ at 298.15 and 310.15 K (25 and 37 °C), respectively.

822

823 3.3. Forces and fluxes in physics and irreversible thermodynamics

824 According to its definition in physics, a potential difference and as such the
 825 *protonmotive force*, Δp_{H^+} , is not a force *per se* (Cohen *et al.* 2008). The fundamental forces of
 826 physics are distinguished from *motive forces* of statistical and irreversible thermodynamics.
 827 Complementary to the attempt towards unification of fundamental forces defined in physics,
 828 the concepts of Nobel laureates Lars Onsager, Erwin Schrödinger, Ilya Prigogine and Peter
 829 Mitchell (even if expressed in apparently unrelated terms) unite the diversity of *generalized* or
 830 ‘isomorphic’ *flux-force* relationships, the product of which links to the dissipation function and
 831 Second Law of thermodynamics (Schrödinger 1944; Prigogine 1967). A *motive force* is the
 832 derivative of potentially available or ‘free’ energy (exergy) per isomorphic *motive* unit (**Box 3**).
 833 Perhaps the first account of a *motive force* in energy transformation can be traced back to the
 834 Peripatetic school around 300 BC in the context of moving a lever, up to Newton’s motive force
 835 proportional to the alteration of motion (Coopersmith 2010).

836 **Vectorial and scalar forces, and fluxes:** In chemical reactions and osmotic or diffusion
 837 processes occurring in a closed heterogeneous system, such as a chamber containing isolated
 838 mitochondria, scalar transformations occur without measured spatial direction but between
 839 separate compartments (translocation between the matrix and intermembrane space) or between

840 energetically-separated chemical substances (reactions from substrates to products). Hence, the
841 corresponding fluxes are not vectorial but scalar, and are expressed per volume and not per
842 membrane area (**Box 2**). The corresponding motive forces are also scalar potential *differences*
843 across the membrane (**Table 5**), without taking into account the *gradients* across the 6 nm thick
844 inner mitochondrial membrane (Rich 2003).

845 **Coupling:** In energetics (ergodynamics), coupling is defined as an exergy transformation
846 fuelled by an exergonic (downhill) input process driving the advancement of an endergonic
847 (uphill) output process. The (negative) output/input power ratio is the efficiency of a coupled
848 energy transformation (**Box 4**). At the limit of maximum efficiency of a completely coupled
849 system, the (negative) input power equals the (positive) output power, such that the total power
850 approaches zero at the maximum efficiency of 1, and the process becomes fully reversible
851 without any dissipation of exergy, *i.e.* without entropy production.

852

853 **Box 4: Coupling, power and efficiency, at constant temperature and pressure**

854 Energetic coupling means that two processes of energy transformation are linked such that the
855 input power, P_{in} , is the driving element of the output power, P_{out} , and the out/input power ratio
856 is the efficiency. In general, power is work per unit time [$J \cdot s^{-1} = W$]. When describing a system
857 with volume V without information on the internal structure, the output is defined as the *external*
858 work (exergy) performed by the *total* system on its environment. Such a system may be open
859 for any type of exchange, or closed and thus allowing only heat and work to be exchanged
860 across the system boundaries. This is the classical black box approach of thermodynamics. In
861 contrast, in a colourful compartmental analysis of *internal* energy transformations (**Fig. 2**), the
862 system is structured and described by definition of ergodynamic compartments (with
863 information on the heterogeneity of the system; **Box 2**) and analysis of separate parts, *i.e.* a
864 sequence of *partial* energy transformations, tr . In general, power per unit volume, P_{tr}/V [$W \cdot L^{-1}$],
865 is the product of a volume-specific flux, J_{tr} , and its conjugated force, F_{tr} , and is closely linked

866 to the dissipation function using the terminology of irreversible thermodynamics (Prigogine
867 1967; Gnaiger 1993a,b). Output power of proton translocation and catabolic input power are
868 (Fig. 2),

869 Output:
$$P_{H^+,out}/V = J_{H^+,out} \cdot F_{H^+,out}$$

870 Input:
$$P_k/V = J_{O_2,k} \cdot F_{O_2,k}$$

871 $F_{O_2,k}$ is the exergonic input force with a negative sign, and, $F_{H^+,out}$, is the endergonic output
872 force with a positive sign (Box 3). Ergodynamic efficiency is the ratio of output/input power,
873 or the flux ratio times force ratio (Gnaiger 1993a,b),

874
$$\varepsilon = \frac{P_{H^+,out}}{-P_k} = \frac{J_{H^+,out}}{J_{O_2,k}} \cdot \frac{F_{H^+,out}}{-F_{O_2,k}}$$

875 The concept of incomplete coupling relates exclusively to the first term, *i.e.* the flux ratio, or
876 H^+_{out}/O_2 ratio (Fig. 1). Likewise, respirometric definitions of the P_{\gg}/O_2 ratio and biochemical
877 coupling efficiency (Section 3.2) consider flux ratios. In a completely coupled process, the
878 power efficiency, ε , depends entirely on the force ratio, ranging from zero efficiency at an
879 output force of zero, to the limiting output force and maximum efficiency of 1.0, when the total
880 power of the coupled process, $P_{\tau} = P_k + P_{H^+,out}$, equals zero, and any net flows are zero at
881 ergodynamic equilibrium of a coupled process. Thermodynamic equilibrium is defined as the
882 state when all potentials (all forces) are dissipated and equilibrate towards their minima of zero.
883 In a fully or completely coupled process, output and input fluxes are directly proportional in a
884 fixed ratio technically defined as a stoichiometric relationship (a gear ratio in a mechanical
885 system). Such maximal stoichiometric output/input flux ratios are considered in OXPHOS
886 analysis as the upper limits or mechanistic H^+_{out}/O_2 and P_{\gg}/O_2 ratios (Fig. 1).

887

888 **Coupled versus bound processes:** Since the chemiosmotic theory describes the
889 mechanisms of coupling in OXPHOS, it may be interesting to ask if the electrical and chemical
890 parts of proton translocation are coupled processes. This is not the case according to the

891 definition of coupling. If the coupling mechanism is disengaged, the output process becomes
 892 independent of the input process, and both proceed in their downhill (exergonic) direction (**Fig.**
 893 **2**). It is not possible to physically uncouple the electrical and chemical processes, which are
 894 only *theoretically* partitioned as electrical and chemical components and can be measured
 895 separately. If partial processes are non-separable, *i.e.*, cannot be uncoupled, then these are not
 896 *coupled* but are defined as *bound* processes. The electrical and chemical parts are tightly bound
 897 partial forces of the protonmotive force, since a flux cannot be partitioned but expressed only
 898 in either an electrical or chemical isomorphic format (**Table 4**).

899

900 **4. Normalization: fluxes and flows**

901 The challenges of measuring mitochondrial respiratory flux are matched by those of
 902 normalization, whereby O₂ consumption may be considered as the nominator and normalization
 903 as the complementary denominator, which are tightly linked in reporting the measurements in
 904 a format commensurate with the requirements of a database.

905

906 *4.1. Flux per chamber volume*

907 When the reactor volume does not change during the reaction, which is typical for liquid
 908 phase reactions, the volume-specific *flux of a chemical reaction* r is the time derivative of the
 909 advancement of the reaction per unit volume, $J_{V,B} = d_r \zeta_B / dt \cdot V^{-1}$ [(mol·s⁻¹)·L⁻¹]. The *rate of*
 910 *concentration change* is dc_B/dt [(mol·L⁻¹)·s⁻¹], where concentration is $c_B = n_B/V$. It is helpful to
 911 make the subtle distinction between [mol·s⁻¹·L⁻¹] and [mol·L⁻¹·s⁻¹] for the fundamentally
 912 different quantities of volume-specific flux and rate of concentration change, which merge to a
 913 single expression only in closed systems. In open systems, external fluxes (such as O₂ supply)
 914 are distinguished from internal transformations (metabolic flux, O₂ consumption). In a closed
 915 system, external flows of all substances are zero and O₂ consumption (internal flow), I_{O_2}
 916 [pmol·s⁻¹], causes a decline of the amount of O₂ in the system, n_{O_2} [nmol]. Normalization of

917 these quantities for the volume of the system, V [$\text{L}=\text{dm}^3$], yields volume-specific O_2 flux,
918 $J_{V,\text{O}_2}=I_{\text{O}_2}/V$ [$\text{nmol}\cdot\text{s}^{-1}\cdot\text{L}^{-1}$], and O_2 concentration, $[\text{O}_2]$ or $c_{\text{O}_2}=n_{\text{O}_2}/V$ [$\text{nmol}\cdot\text{mL}^{-1}=\mu\text{mol}\cdot\text{L}^{-1}=\mu\text{M}$].
919 Instrumental background O_2 flux is due to external flux into a non-ideal closed respirometer,
920 such that total volume-specific flux has to be corrected for instrumental background O_2 flux,
921 *i.e.* O_2 diffusion into or out of the instrumental chamber. J_{V,O_2} is relevant mainly for
922 methodological reasons and should be compared with the accuracy of instrumental resolution
923 of background-corrected flux, *e.g.* $\pm 1 \text{ nmol}\cdot\text{s}^{-1}\cdot\text{L}^{-1}$ (Gnaiger 2001). ‘Metabolic’ or catabolic
924 indicates O_2 flux, $J_{\text{O}_2,\text{k}}$, corrected for instrumental background O_2 flux and chemical background
925 O_2 flux due to autoxidation of chemical components added to the incubation medium.

926

927 4.2. System-specific and sample-specific normalization

928 Application of common and generally defined units is required for direct transfer of
929 reported results into a database. The second [s] is the *SI* unit for the base quantity *time*. It is also
930 the standard time-unit used in solution chemical kinetics. **Table 6** lists some conversion factors
931 to obtain *SI* units. The term *rate* is not sufficiently defined to be useful for a database (**Fig. 7**).
932 The inconsistency of the meanings of rate becomes fully apparent when considering Galileo
933 Galilei’s famous principle, that ‘bodies of different weight all fall at the same rate (have a
934 constant acceleration)’ (Coopersmith 2010).

935 **Extensive quantities:** An extensive quantity increases proportionally with system size.
936 The magnitude of an extensive quantity is completely additive for non-interacting subsystems,
937 such as mass or flow expressed per defined system. The magnitude of these quantities depends
938 on the extent or size of the system (Cohen *et al.* 2008).

939

940 **Fig. 7. Different meanings of rate**941 **may lead to confusion, if the**942 **normalization is not sufficiently**943 **specified.** Results are frequently944 expressed as mass-specific *flux*, J_m ,

945 per mg protein, dry or wet weight

946 (mass). Cell volume, V_{cell} , or947 mitochondrial volume, V_{mt} , may be

948 used for normalization (volume-

949 specific flux, $J_{V_{\text{cell}}}$ or $J_{V_{\text{mt}}}$), which then must be clearly distinguished from flux, J_V , expressed for950 methodological reasons per volume of the measurement system, or flow per cell, I_x .

951

952 **Size-specific quantities:** ‘The adjective *specific* before the name of an extensive quantity953 is often used to mean *divided by mass*’ (Cohen *et al.* 2008). Mass-specific flux is flow divided

954 by mass of the system. A mass-specific quantity is independent of the extent of non-interacting

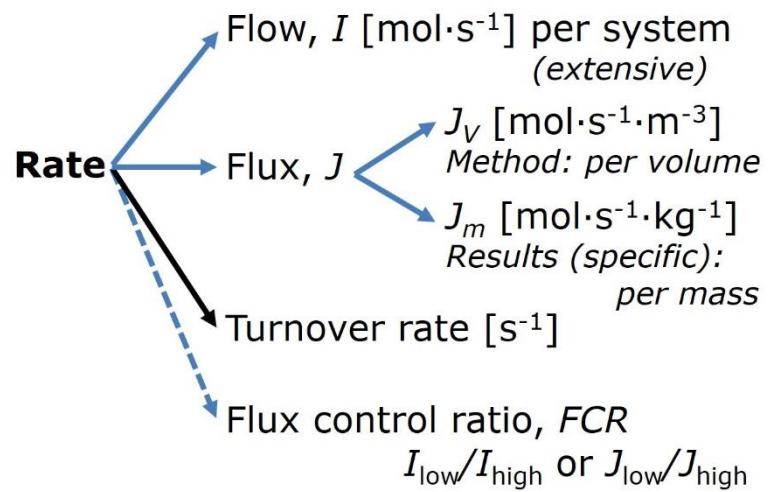
955 homogenous subsystems. Tissue-specific quantities are of fundamental interest in comparative

956 mitochondrial physiology, where *specific* refers to the *type* rather than *mass* of the tissue. The957 term *specific*, therefore, must be further clarified, such that tissue mass-specific, *e.g.*, muscle

958 mass-specific quantities are defined.

959 **Molar quantities:** ‘The adjective *molar* before the name of an extensive quantity960 generally means *divided by amount of substance*’ (Cohen *et al.* 2008). The notion that all molar961 quantities then become *intensive* causes ambiguity in the meaning of *molar Gibbs energy*. It is

962 important to emphasize the fundamental difference between normalization for amount of

963 substance *in a system* or for amount of motive substance *in a transformation*. When the Gibbs964 energy of a system, G [J], is divided by the amount of substance B in the system, n_B [mol], a965 *size-specific* molar quantity is obtained, $G_B = G/n_B$ [J·mol⁻¹], which is not any force at all. In966 contrast, when the partial Gibbs energy change, $\partial_r G$ [J], is divided by the motive amount of

951

952 **Size-specific quantities:** ‘The adjective *specific* before the name of an extensive quantity953 is often used to mean *divided by mass*’ (Cohen *et al.* 2008). Mass-specific flux is flow divided

954 by mass of the system. A mass-specific quantity is independent of the extent of non-interacting

955 homogenous subsystems. Tissue-specific quantities are of fundamental interest in comparative

956 mitochondrial physiology, where *specific* refers to the *type* rather than *mass* of the tissue. The957 term *specific*, therefore, must be further clarified, such that tissue mass-specific, *e.g.*, muscle

958 mass-specific quantities are defined.

959 **Molar quantities:** ‘The adjective *molar* before the name of an extensive quantity960 generally means *divided by amount of substance*’ (Cohen *et al.* 2008). The notion that all molar961 quantities then become *intensive* causes ambiguity in the meaning of *molar Gibbs energy*. It is

962 important to emphasize the fundamental difference between normalization for amount of

963 substance *in a system* or for amount of motive substance *in a transformation*. When the Gibbs964 energy of a system, G [J], is divided by the amount of substance B in the system, n_B [mol], a965 *size-specific* molar quantity is obtained, $G_B = G/n_B$ [J·mol⁻¹], which is not any force at all. In966 contrast, when the partial Gibbs energy change, $\partial_r G$ [J], is divided by the motive amount of

967 substance B in reaction r (advancement of reaction), $\partial_r \zeta_B$ [mol], the resulting intensive molar
 968 quantity, $F_{r,B} = \partial G / \partial_r \zeta_B$ [$\text{J} \cdot \text{mol}^{-1}$], is the chemical motive force of reaction r involving 1 mol B
 969 (**Table 5**, Note 4).

970 **Flow per system, I :** In analogy to electrical terms, flow as an extensive quantity (I ; per
 971 system) is distinguished from flux as a size-specific quantity (J ; per system size) (**Fig. 7**).
 972 Electric current is flow, I_{el} [$\text{A} = \text{C} \cdot \text{s}^{-1}$] per system (extensive quantity). When dividing this
 973 extensive quantity by system size (membrane area), a size-specific quantity is obtained, which
 974 is electric flux (electric current density), J_{el} [$\text{A} \cdot \text{m}^{-2} = \text{C} \cdot \text{s}^{-1} \cdot \text{m}^{-2}$].

975 **Size-specific flux, J :** Metabolic O_2 flow per tissue increases as tissue mass is increased.
 976 Tissue mass-specific O_2 flux should be independent of the size of the tissue sample studied in
 977 the instrument chamber, but volume-specific O_2 flux (per volume of the instrument chamber,
 978 V) should increase in direct proportion to the amount of sample in the chamber. Accurate
 979 definition of the experimental system is decisive: whether the experimental chamber is the
 980 closed, open, isothermal or non-isothermal *system* with defined volume as part of the
 981 measurement apparatus, in contrast to the experimental *sample* in the chamber (**Table 6**).
 982 Volume-specific O_2 flux depends on mass-concentration of the sample in the chamber, but
 983 should be independent of the chamber volume. There are practical limitations to increasing the
 984 mass-concentration of the sample in the chamber, when one is concerned about crowding
 985 effects and instrumental time resolution.

986 **Sample concentration C_{mX} :** Normalization for sample concentration is required for
 987 reporting respiratory data. Consider a tissue or cells as the sample, X , and the sample mass, m_X
 988 [mg] from which a mitochondrial preparation is obtained. The sample mass is frequently
 989 measured as wet or dry weight ($m_X \equiv W_w$ or W_d [mg]), or as amount of tissue or cell protein
 990 ($m_X \equiv m_{\text{Protein}}$). In the case of permeabilized tissues, cells, and homogenates, the sample
 991 concentration, $C_{mX} = m_X / V$ [$\text{mg} \cdot \text{mL}^{-1} = \text{g} \cdot \text{L}^{-1}$], is simply the mass of the subsample of tissue that is
 992 transferred into the instrument chamber. Part of the mitochondria from the tissue is lost during

993 preparation of isolated mitochondria, and only a fraction of mitochondria is obtained, expressed
 994 as the mitochondrial yield (**Fig. 8**). At a high mitochondrial yield the sample of isolated
 995 mitochondria is more representative of the total mitochondrial population than in preparations
 996 characterized by low mitochondrial yield. Determination of the mitochondrial yield is based on
 997 measurement of the concentration of a mitochondrial marker in the tissue homogenate, $C_{mte,thom}$,
 998 which simultaneously provides information on the specific mitochondrial density in the sample
 999 (**Fig. 8**).

1000 Tissues can contain multiple cell populations which may have distinct mitochondrial
 1001 subtypes. Mitochondria are also in a constant state of flux due to highly dynamic fission and
 1002 fusion cycles, and can exist in multiple stages and sizes which may be altered by a range of
 1003 factors. The isolation of mitochondria (often achieved through differential centrifugation) can
 1004 therefore yield a subsample of the mitochondrial types present in a tissue, dependent on
 1005 isolation protocols utilized (*e.g.* centrifugation speed). This possible artefact should be taken
 1006 into account when planning experiments using isolated mitochondria. The tendency for
 1007 mitochondria of specific sizes to be enriched at different centrifugation speeds also has the
 1008 potential to allow the isolation of specific mitochondrial subpopulations and therefore the
 1009 analysis of mitochondria from multiple cell lineages within a single tissue.

1010 **Mass-specific flux, J_{mX,O_2} :** Mass-specific flux is obtained by expressing respiration per
 1011 mass of sample, m_X [mg]. X is the type of sample, *e.g.*, tissue homogenate, permeabilized fibres
 1012 or cells. Volume-specific flux is divided by mass concentration of X , $J_{mX,O_2} = J_{V,O_2}/C_{mX}$; or flow
 1013 per cell is divided by mass per cell, $J_{mcell,O_2} = I_{cell,O_2}/M_{cell}$. If mass-specific O_2 flux is constant
 1014 and independent of sample size (expressed as mass), then there is no interaction between the
 1015 subsystems. A 1.5 mg and a 3.0 mg muscle sample respire at identical mass-specific flux.
 1016 Mass-specific O_2 flux, however, may change with the mass of a tissue sample, cells or isolated
 1017 mitochondria in the measuring chamber, in which case the nature of the interaction becomes an
 1018 issue. Optimization of cell density and arrangement is generally important and particularly in

1019 experiments carried out in wells, considering the confluency of the cell monolayer or clumps
 1020 of cells (Salabei *et al.* 2014).

1021

1022 **Table 6. Sample concentrations and normalization of flux with SI base units.**

Expression	Symbol	Definition	SI Unit	Notes
Sample				
Identity of sample	X	Cells, animals, patients		
Number of sample entities X	N_X	Number of cells, <i>etc.</i>	x	
Mass of sample X	m_X		kg	1
Mass of entity X	M_X	$M_X = m_X \cdot N_X^{-1}$	$\text{kg} \cdot \text{x}^{-1}$	1
Mitochondria				
Mitochondria	mt	$X = \text{mt}$		
Amount of mt-elements	mte	Quantity of mt-marker	x_{mte}	
Concentrations				
Sample number concentration	C_{NX}	$C_{NX} = N_X \cdot V^{-1}$	$\text{x} \cdot \text{m}^{-3}$	2
Sample mass concentration	C_{mX}	$C_{mX} = m_X \cdot V^{-1}$	$\text{kg} \cdot \text{m}^{-3}$	
Mitochondrial concentration	C_{mte}	$C_{\text{mte}} = \text{mte} \cdot V^{-1}$	$x_{\text{mte}} \cdot \text{m}^{-3}$	3
Specific mitochondrial density	D_{mte}	$D_{\text{mte}} = \text{mte} \cdot m_X^{-1}$	$x_{\text{mte}} \cdot \text{kg}^{-1}$	4
Mitochondrial content, mte per entity X	mte_X	$\text{mte}_X = \text{mte} \cdot N_X^{-1}$	$x_{\text{mte}} \cdot \text{x}^{-1}$	5
O₂ flow and flux				
Flow	I_{O_2}	Internal flow	$\text{mol} \cdot \text{s}^{-1}$	6
Volume-specific flux	J_{V,O_2}	$J_{V,\text{O}_2} = I_{\text{O}_2} \cdot V^{-1}$	$\text{mol} \cdot \text{s}^{-1} \cdot \text{m}^{-3}$	7
Flow per sample entity X	I_{X,O_2}	$I_{X,\text{O}_2} = J_{V,\text{O}_2} \cdot C_{NX}^{-1}$	$\text{mol} \cdot \text{s}^{-1} \cdot \text{x}^{-1}$	8
Mass-specific flux	J_{mX,O_2}	$J_{mX,\text{O}_2} = J_{V,\text{O}_2} \cdot C_{mX}^{-1}$	$\text{mol} \cdot \text{s}^{-1} \cdot \text{kg}^{-1}$	9
Mitochondria-specific flux	$J_{\text{mte},\text{O}_2}$	$J_{\text{mte},\text{O}_2} = J_{V,\text{O}_2} \cdot C_{\text{mte}}^{-1}$	$\text{mol} \cdot \text{s}^{-1} \cdot x_{\text{mte}}^{-1}$	10

1024

1025 1 The SI prefix k is used for the SI base unit of mass (kg=1,000 g). In praxis, various SI prefixes are
 1026 used for convenience, to make numbers easily readable, e.g. 1 mg tissue, cell or mitochondrial mass
 1027 instead of 0.000001 kg.

1028 2 In case $X = \text{cells}$, the sample number concentration is $C_{N_{\text{cell}}} = N_{\text{cell}} \cdot V^{-1}$, and volume may be expressed
 1029 in [dm³=L] or [cm³=mL]. See Table 7 for different sample types.

1030 3 mt-concentration is an experimental variable, dependent on sample concentration: (1) $C_{\text{mte}} = \text{mte} \cdot V^{-1}$;
 1031 (2) $C_{\text{mte}} = \text{mte}_X \cdot C_{NX}$; (3) $C_{\text{mte}} = C_{mX} \cdot D_{\text{mte}}$.

1032 4 If the amount of mitochondria, mte, is expressed as mitochondrial mass, then D_{mte} is the mass
 1033 fraction of mitochondria in the sample. If mte is expressed as mitochondrial volume, V_{mt} , and the

1034 mass of sample, m_X , is replaced by volume of sample, V_X , then D_{mte} is the volume fraction of
 1035 mitochondria in the sample.

1036 5 $mte_X = mte \cdot N_X^{-1} = C_{mte} \cdot C_{NX}^{-1}$.

1037 6 Entity O_2 can be replaced by other chemical entities B to study different reactions.

1038 7 l_{O_2} and V are defined per instrument chamber as a system of constant volume (and constant
 1039 temperature), which may be closed or open. l_{O_2} is abbreviated for $l_{O_2,r}$, i.e. the metabolic or internal
 1040 O_2 flow of the chemical reaction r in which O_2 is consumed, hence the negative stoichiometric
 1041 number, $\nu_{O_2} = -1$. $l_{O_2,r} = drn_{O_2}/dt \nu_{O_2}^{-1}$. If r includes all chemical reactions in which O_2 participates, then
 1042 $drn_{O_2} = dn_{O_2} - d_e n_{O_2}$, where dn_{O_2} is the change in the amount of O_2 in the instrument chamber and
 1043 $d_e n_{O_2}$ is the amount of O_2 added externally to the system. At steady state, by definition $dn_{O_2} = 0$, hence
 1044 $drn_{O_2} = -d_e n_{O_2}$.

1045 8 J_{V,O_2} is an experimental variable, expressed per volume of the instrument chamber.

1046 9 l_{X,O_2} is a physiological variable, depending on the size of entity X .

1047 10 There are many ways to normalize for a mitochondrial marker, that are used in different experimental
 1048 approaches: (1) $J_{mte,O_2} = J_{V,O_2} \cdot C_{mte}^{-1}$; (2) $J_{mte,O_2} = J_{V,O_2} \cdot C_{mX}^{-1} \cdot D_{mte}^{-1} = J_{mX,O_2} \cdot D_{mte}^{-1}$; (3) $J_{mte,O_2} =$
 1049 $J_{V,O_2} \cdot C_{NX}^{-1} \cdot mte_X^{-1} = l_{X,O_2} \cdot mte_X^{-1}$; (4) $J_{mte,O_2} = l_{O_2} \cdot mte^{-1}$.

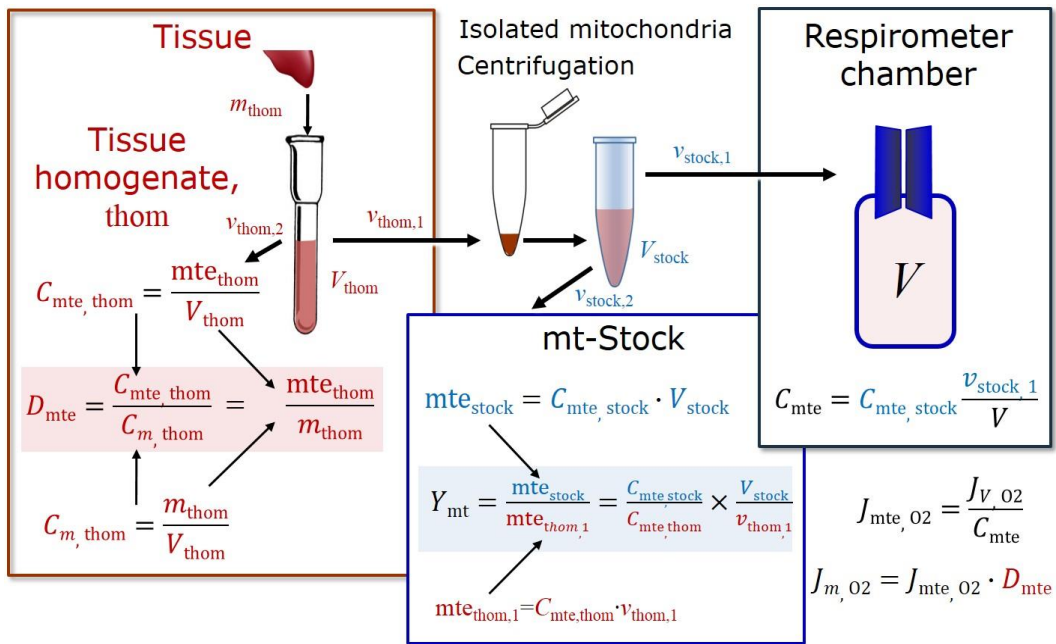
1050

1051

1052

1053

1054



1055

Symbol	Definition [Units]
C_{mte}	Mitochondrial concentration in chamber [$x_{mte} \cdot L^{-1}$]
C_m	Sample mass concentration in chamber [$g \cdot L^{-1}$]
D_{mte}	Specific mte-density per tissue mass [$x_{mte} \cdot g^{-1}$]
J_{m,O_2}	Mass-specific O_2 flux [$nmol \cdot s^{-1} \cdot g^{-1}$]
J_{mte,O_2}	Mitochondria-specific O_2 flux [$nmol \cdot s^{-1} \cdot x_{mte}^{-1}$]
mte	Amount of mitochondrial elements [x_{mte}]
m_{thom}	Mass of tissue in the homogenate [g]
Y_{mt}	Yield of isolated mitochondria

1056

1057

1058

1059

1060

1061

1062

1063

1064

1065

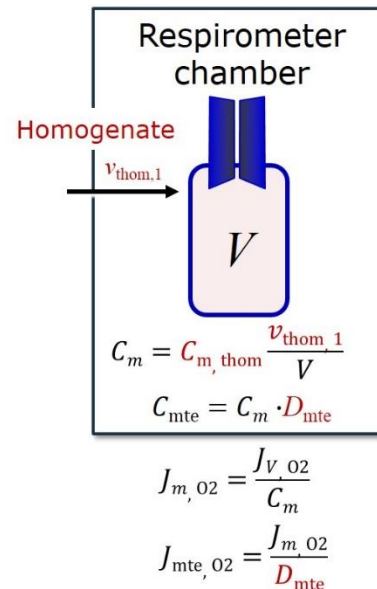


Fig. 8. Normalization of volume-specific flux of isolated mitochondria and tissue

homogenate. A: Mitochondrial yield, Y_{mt} , in preparation of isolated mitochondria. $v_{thom,1}$

and $v_{stock,1}$ are the volumes transferred from the total volume, V_{thom} and V_{stock} , respectively.

$mte_{thom,1}$ is the amount of mitochondrial elements in volume $v_{thom,1}$ used for isolation. **B:**

In respirometry with homogenate, $v_{thom,1}$ is transferred directly into the respirometer

chamber. See **Table 6** for further explanation of symbols.

1066 **Table 7. Some useful abbreviations**
 1067 **of various sample types, X.**

1068	<hr/>	
1069	Identity of sample	X
1070	<hr/>	
1071	Mitochondrial preparations	mtprep
1072	Isolated mitochondria	imt
1073	Tissue homogenate	thom
1074	Permeabilized tissue	pti
1075	Permeabilized fibres	pfi
1076	Permeabilized cells	pce
1077	Cells	ce
1078	<hr/>	
1079		

1080 **Number concentration, C_{NX} :** The experimental *number concentration* of sample in the
 1081 case of cells or animals, *e.g.*, nematodes is $C_{NX}=N_X/V$ [$x \cdot mL^{-1}$], where N_X is the number of cells
 1082 or organisms in the chamber (**Table 6**).

1083 **Flow per sample entity, I_{X,O_2} :** A special case of normalization is encountered in
 1084 respiratory studies with permeabilized (or intact) cells. If respiration is expressed per cell, the
 1085 O_2 flow per measurement system is replaced by the O_2 flow per cell, I_{cell,O_2} (**Table 6**). O_2 flow
 1086 can be calculated from volume-specific O_2 flux, J_{V,O_2} [$nmol \cdot s^{-1} \cdot L^{-1}$] (per V of the measurement
 1087 chamber [L]), divided by the number concentration of cells, $C_{N_{ce}}=N_{ce}/V$ [$cell \cdot L^{-1}$], where N_{ce} is
 1088 the number of cells in the chamber. Cellular O_2 flow can be compared between cells of identical
 1089 size. To take into account changes and differences in cell size, further normalization is required
 1090 to obtain cell size-specific or mitochondrial marker-specific O_2 flux (Renner *et al.* 2003).

1091 The complexity changes when the sample is a whole organism studied as an experimental
 1092 model. The well-established scaling law in respiratory physiology reveals a strong interaction
 1093 of O_2 consumption and individual body mass of an organism, since *basal* metabolic rate (flow)
 1094 does not increase linearly with body mass, whereas *maximum* mass-specific O_2 flux, \dot{V}_{O_2max} or

1095 $\dot{V}_{O_{2peak}}$, is approximately constant across a large range of individual body mass (Weibel and
1096 Hoppeler 2005), with individuals, breeds, and certain species deviating substantially from this
1097 general relationship. $\dot{V}_{O_{2peak}}$ of human endurance athletes is 60 to 80 mL O₂·min⁻¹·kg⁻¹ body
1098 mass, converted to $J_{m,O_{2peak}}$ of 45 to 60 nmol·s⁻¹·g⁻¹ (Gnaiger 2014; **Table 8**).

1099

1100 *4.3. Normalization for mitochondrial content*

1101 Normalization is a problematic subject and it is essential to consider the question of the
1102 study. If the study aims to compare tissue performance, such as the effects of a certain treatment
1103 on a specific tissue, then normalization can be successful, using tissue mass or protein content,
1104 for example. If the aim, however, is to find differences of mitochondrial function independent
1105 of mitochondrial density (**Table 6**), then normalization to a mitochondrial marker is imperative.
1106 However, one cannot assume that quantitative changes in various markers such as
1107 mitochondrial proteins necessarily occur in parallel with one another. It is important to first
1108 establish that the marker chosen is not selectively altered by the performed treatment. In
1109 conclusion, the normalization must reflect the question under investigation to reach a satisfying
1110 answer. On the other hand, the goal of comparing results across projects and institutions
1111 requires some standardization on normalization for entry into a databank.

1112 **Mitochondrial concentration, C_{mte} , and mitochondrial markers:** It is important that
1113 mitochondrial content in the tissue and the measurement chamber be quantified, as a
1114 physiological output and result of mitochondrial biogenesis and degradation, and as a quantity
1115 for normalization in functional analyses. Mitochondrial organelles comprise a cellular
1116 reticulum that is in a continual flux of fusion and fission. Hence the definition of an "amount"
1117 of mitochondria is often misconceived: mitochondria cannot be counted as a number of
1118 occurring elements. Therefore, quantification of the "amount" of mitochondria depends on
1119 measurement of chosen mitochondrial markers. 'Mitochondria are the structural and functional
1120 elemental units of cell respiration' (Gnaiger 2014). The quantity of a mitochondrial marker can

1121 be considered as the measurement of the amount of *elemental mitochondrial units* or
 1122 *mitochondrial elements*, mte. However, since mitochondrial quality changes under certain
 1123 stimuli, particularly in mitochondrial dysfunction, some markers can vary while other markers
 1124 are unchanged. (1) Mitochondrial volume or membrane area are structural markers, whereas
 1125 mitochondrial protein mass is frequently used as a marker for isolated mitochondria. (2)
 1126 Mitochondrial marker enzymes (amounts or activities) and molecular markers can be selected
 1127 as matrix markers, *e.g.*, citrate synthase activity, mtDNA; or inner mt-membrane markers, *e.g.*,
 1128 cytochrome *c* oxidase activity, *aa*₃ content, cardiolipin, TOM20. (3) Extending the
 1129 measurement of mitochondrial marker enzyme activity to mitochondrial pathway capacity,
 1130 measured as ET or OXPHOS capacity, can be considered as an integrative functional
 1131 mitochondrial marker.

1132 Depending on the type of mitochondrial marker, the mitochondrial elements, mte, are
 1133 expressed in marker-specific units. Although concentration and density are used synonymously
 1134 in physical chemistry, it is recommended to distinguish *experimental mitochondrial*
 1135 *concentration*, $C_{\text{mte}} = \text{mte}/V$ and *physiological mitochondrial density*, $D_{\text{mte}} = \text{mte}/m_X$. Then
 1136 mitochondrial density is the amount of mitochondrial elements per mass of tissue. The former
 1137 is mitochondrial density multiplied by sample mass concentration, $C_{\text{mte}} = D_{\text{mte}} \cdot C_{m_X}$, or
 1138 mitochondrial content multiplied by sample number concentration, $C_{\text{mte}} = \text{mte}_X \cdot C_{N_X}$ (**Table 6**).

1139 **Mitochondria-specific flux, $J_{\text{mte},\text{O}_2}$:** Volume-specific metabolic O₂ flux depends on: (1)
 1140 the sample concentration in the volume of the instrument chamber, C_{m_X} , or C_{N_X} ; (2) the
 1141 mitochondrial density in the sample, $D_{\text{mte}} = \text{mte}/m_X$ or $\text{mte}_X = \text{mte}/N_X$; and (3) the specific
 1142 mitochondrial activity or performance per elemental mitochondrial unit, $J_{\text{mte},\text{O}_2} = J_{V,\text{O}_2}/C_{\text{mte}}$
 1143 (**Table 6**). Obviously, the numerical results for $J_{\text{mte},\text{O}_2}$ vary according to the type of
 1144 mitochondrial marker chosen for measurement of mte and $C_{\text{mte}} = \text{mte}/V$. Some problems are
 1145 common for all mitochondrial markers: (1) Accuracy of measurement is crucial, since even a
 1146 highly accurate and reproducible measurement of O₂ flux becomes inaccurate and noisy if

1147 normalized for a biased and noisy measurement of a mitochondrial marker. This problem is
1148 acute in mitochondrial respiration because the denominators used (the mitochondrial marker)
1149 are often very small moieties whose accurate and precise determination is difficult. This
1150 problem can be avoided when O₂ fluxes measured in substrate-uncoupler-inhibitor titration
1151 protocols are normalized for flux in a defined respiratory reference state, which is used as an
1152 *internal* marker and yields flux control ratios, *FCRs* (**Fig. 7**). *FCRs* are independent of any
1153 *externally* measured markers and, therefore, are statistically very robust. *FCRs* indicate
1154 qualitative changes of mitochondrial respiratory control, with highest quantitative resolution,
1155 separating the effect of mitochondrial density or concentration on J_{mX,O_2} or I_{X,O_2} from that of
1156 function per elemental mitochondrial marker, J_{mte,O_2} (Pesta *et al.* 2011; Gnaiger 2014). (2) If
1157 mitochondrial quality does not change and only the amount of mitochondria, defined by the
1158 chosen mitochondrial marker, varies as a determinant of mass-specific flux, then any marker is
1159 equally qualified and selection of the optimum marker depends only on the accuracy and
1160 precision of measurement of the mitochondrial marker. (3) If mitochondrial flux control ratios
1161 change, then there may not be any best mitochondrial marker. In general, measurement of
1162 multiple mitochondrial markers enables a comparison and evaluation of normalization for a
1163 variety of mitochondrial markers.

1164

1165 4.4. Conversion: units and normalization

1166 Many different units have been used to report the rate of oxygen consumption, OCR
1167 (**Table 8**). *SI* base units provide the common reference for introducing the theoretical principles
1168 (**Fig. 7**), and are used with appropriately chosen *SI* prefixes to express numerical data in the
1169 most practical format, with an effort towards unification within specific areas of application
1170 (**Table 9**). For studies of cells, we recommend that respiration be expressed, as far as possible,
1171 as (1) O₂ flux normalized for a mitochondrial marker, for separation of the effects of
1172 mitochondrial quality and content on cell respiration (this includes *FCRs* as a normalization for

1173 a functional mitochondrial marker); (2) O₂ flux in units of cell volume or mass, for comparison
 1174 of respiration of cells with different cell size (Renner *et al.* 2003) and with studies on tissue
 1175 preparations, and (3) O₂ flow in units of attomole (10⁻¹⁸ mol) of O₂ consumed by each cell in a
 1176 second [amol·s⁻¹·cell⁻¹], numerically equivalent to [pmol·s⁻¹·10⁻⁶ cells]. This convention allows
 1177 information to be easily used when designing experiments in which oxygen consumption must
 1178 be considered. For example, to estimate the volume-specific O₂ flux in an instrument chamber
 1179 that would be expected at a particular cell number concentration, one simply needs to multiply
 1180 the flow per cell by the number of cells per volume of interest. This provides the amount of O₂
 1181 [mol] consumed per time [s⁻¹] per unit volume [L⁻¹]. At an O₂ flow of 100 amol·s⁻¹·cell⁻¹ and a
 1182 cell density of 10⁹ cells·L⁻¹ (10⁶ cells·mL⁻¹), the volume-specific O₂ flux is 100 nmol·s⁻¹·L⁻¹ (100
 1183 pmol·s⁻¹·mL⁻¹).

1184

1185 **Table 8. Conversion of various units used in respirometry and**
 1186 **ergometry.** *e* is the number of electrons or reducing equivalents. *z_B* is the
 1187 charge number of entity B.

1188

1 Unit	x	Multiplication factor	SI-Unit	Note
ng.atom O·s ⁻¹	(2 e)	0.5	nmol O ₂ ·s ⁻¹	
ng.atom O·min ⁻¹	(2 e)	8.33	pmol O ₂ ·s ⁻¹	
natom O·min ⁻¹	(2 e)	8.33	pmol O ₂ ·s ⁻¹	
nmol O ₂ ·min ⁻¹	(4 e)	16.67	pmol O ₂ ·s ⁻¹	
nmol O ₂ ·h ⁻¹	(4 e)	0.2778	pmol O ₂ ·s ⁻¹	
mL O ₂ ·min ⁻¹ at STPD ^a		0.744	μmol O ₂ ·s ⁻¹	1
W = J/s at -470 kJ/mol O ₂		-2.128	μmol O ₂ ·s ⁻¹	
mA = mC·s ⁻¹	(z _{H+} =1)	10.36	nmol H ⁺ ·s ⁻¹	2
mA = mC·s ⁻¹	(z _{O2} =4)	2.59	nmol O ₂ ·s ⁻¹	2
nmol H ⁺ ·s ⁻¹	(z _{H+} =1)	0.09649	mA	3
nmol O ₂ ·s ⁻¹	(z _{O2} =4)	0.38594	mA	3

1189

- 1190 1 At standard temperature and pressure dry (STPD: 0 °C=273.15 K and 1
 1191 atm=101.325 kPa=760 mmHg), the molar volume of an ideal gas, V_m , and V_{m,O_2}
 1192 is 22.414 and 22.392 L.mol⁻¹ respectively. Rounded to three decimal places, both
 1193 values yield the conversion factor of 0.744. For comparison at NTPD (20 °C),
 1194 V_{m,O_2} is 24.038 L.mol⁻¹. Note that the *SI* standard pressure is 100 kPa.
- 1195 2 The multiplication factor is $10^6/(z_B \cdot F)$.
- 1196 3 The multiplication factor is $z_B \cdot F/10^6$.

1197

1198 Although volume is expressed as m³ using the *SI* base unit, the litre [dm³] is the basic unit
 1199 of volume for concentration and is used for most solution chemical kinetics. If one multiplies
 1200 I_{cell,O_2} by C_{Ncell} , then the result will not only be the amount of O₂ [mol] consumed per time [s⁻¹]
 1201 in one litre [L⁻¹], but also the change in the concentration of oxygen per second (for any volume
 1202 of an ideally closed system). This is ideal for kinetic modeling as it blends with chemical rate
 1203 equations where concentrations are typically expressed in mol·L⁻¹ (Wagner *et al.* 2011). In
 1204 studies of multinuclear cells, such as differentiated skeletal muscle cells, it is easy to determine
 1205 the number of nuclei but not the total number of cells. A generalized concept, therefore, is
 1206 obtained by substituting cells by nuclei as the sample entity. This does not hold, however, for
 1207 enucleated platelets.

1208

1209 4.5. Conversion: oxygen, proton and ATP flux

1210 $J_{O_2,k}$ is coupled in mitochondrial steady states to proton cycling, $J_{\infty H^+} = J_{H^+,out} = J_{H^+,in}$ (**Fig.**
 1211 **2**). $J_{H^+,out/n}$ and $J_{H^+,in/n}$ [nmol·s⁻¹·L⁻¹] are converted into electrical units, $J_{H^+,out/e}$
 1212 [mC·s⁻¹·L⁻¹=mA·L⁻¹] = $J_{H^+,out/n}$ [nmol·s⁻¹·L⁻¹]· F [C·mol⁻¹]·10⁻⁶ (**Table 4**). At a $J_{H^+,out}/J_{O_2,k}$ ratio
 1213 or H⁺_{out}/O₂ of 20 (H⁺_{out}/O=10), a volume-specific O₂ flux of 100 nmol·s⁻¹·L⁻¹ would correspond
 1214 to a proton flux of 2,000 nmol H⁺_{out}·s⁻¹·L⁻¹ or volume-specific current of 193 mA·L⁻¹.

1215
$$J_{V,H^+,out/e} [\text{mA} \cdot \text{L}^{-1}] = J_{V,H^+,out/n} \cdot F \cdot 10^{-6} [\text{nmol} \cdot \text{s}^{-1} \cdot \text{L}^{-1} \cdot \text{mC} \cdot \text{nmol}^{-1}] \quad (\text{Eq. 3.1})$$

$$J_{V,H^{+}out/e} [\text{mA}\cdot\text{L}^{-1}] = J_{V,O_2}(\text{H}^{+}_{out}/\text{O}_2)\cdot F\cdot 10^{-6} [\text{mC}\cdot\text{s}^{-1}\cdot\text{L}^{-1}=\text{mA}\cdot\text{L}^{-1}] \quad (\text{Eq. 3.2})$$

1217

1218 **Table 9. Conversion for units with preservation of numerical values.**

Name	Frequently used unit	Equivalent unit	Note
Volume-specific flux, J_{V,O_2}	$\text{pmol}\cdot\text{s}^{-1}\cdot\text{mL}^{-1}$	$\text{nmol}\cdot\text{s}^{-1}\cdot\text{L}^{-1}$	1
	$\text{mmol}\cdot\text{s}^{-1}\cdot\text{L}^{-1}$	$\text{mol}\cdot\text{s}^{-1}\cdot\text{m}^{-3}$	
Cell-specific flow, I_{O_2}	$\text{pmol}\cdot\text{s}^{-1}\cdot 10^{-6}$ cells	$\text{amol}\cdot\text{s}^{-1}\cdot\text{cell}^{-1}$	2
	$\text{pmol}\cdot\text{s}^{-1}\cdot 10^{-9}$ cells	$\text{zmol}\cdot\text{s}^{-1}\cdot\text{cell}^{-1}$	3
Cell number concentration, C_{Nce}	10^6 cells $\cdot\text{mL}^{-1}$	10^9 cells $\cdot\text{L}^{-1}$	
Mitochondrial protein concentration, C_{mte}	0.1 mg $\cdot\text{mL}^{-1}$	0.1 g $\cdot\text{L}^{-1}$	
Mass-specific flux, J_{m,O_2}	$\text{pmol}\cdot\text{s}^{-1}\cdot\text{mg}^{-1}$	$\text{nmol}\cdot\text{s}^{-1}\cdot\text{g}^{-1}$	4
Catabolic power, P_{k,O_2}	$\mu\text{W}\cdot 10^{-6}$ cells	$\text{pW}\cdot\text{cell}^{-1}$	1
Volume	1,000 L	m^3 (1,000 kg)	
	L	dm^3 (kg)	
	mL	cm^3 (g)	
	μL	mm^3 (mg)	
	fL	μm^3 (pg)	
Amount of substance concentration	$\text{M} = \text{mol}\cdot\text{L}^{-1}$	$\text{mol}\cdot\text{dm}^{-3}$	

1219

1220 1 pmol: picomole = 10^{-12} mol1221 2 amol: attomole = 10^{-18} mol1222 3 zmol: zeptomole = 10^{-21} mol1223 4 nmol: nanomole = 10^{-9} mol

1224

1225 ET capacity in various human cell types including HEK 293, primary HUVEC and fibroblasts
1226 ranges from 50 to 180 $\text{amol}\cdot\text{s}^{-1}\cdot\text{cell}^{-1}$, measured in intact cells in the noncoupled state (see
1227 Gnaiger 2014). At 100 $\text{amol}\cdot\text{s}^{-1}\cdot\text{cell}^{-1}$ corrected for ROX (corresponding to a catabolic power
1228 of -48 $\text{pW}\cdot\text{cell}^{-1}$), the current across the mt-membranes, I_e , approximates 193 $\text{pA}\cdot\text{cell}^{-1}$ or 0.2
1229 nA per cell. See Rich (2003) for an extension of quantitative bioenergetics from the molecular
1230 to the human scale, with a transmembrane proton flux equivalent to 520 A in an adult at a
1231 catabolic power of -110 W. Modelling approaches illustrate the link between proton motive
1232 force and currents (Willis *et al.* 2016). For NADH- and succinate-linked respiration, the
1233 mechanistic P_{\gg}/O_2 ratio (referring to the full 4 electron reduction of O_2) is calculated at 20/3.7
1234 and 12/3.7, respectively (Eq. 4) equal to 5.4 and 3.3. The classical P_{\gg}/O ratios (referring to the
1235 2 electron reduction of $0.5 O_2$) are 2.7 and 1.6 (Watt *et al.* 2010), in direct agreement with the

1236 measured P \gg /O ratio for succinate of 1.58 ± 0.02 (Gnaiger *et al.* 2000; for detailed reviews see
 1237 Wikström and Hummer 2012; Sazanov 2015),

$$1238 \quad P_{\gg}/O_2 = (H^+_{out}/O_2)/(H^+_{in}/P_{\gg}) \quad (\text{Eq. 4})$$

1239 In summary (**Fig. 1**),

$$1240 \quad J_{V,P_{\gg}} [\text{nmol}\cdot\text{s}^{-1}\cdot\text{L}^{-1}] = J_{V,O_2}\cdot(H^+_{out}/O_2)/(H^+_{in}/P_{\gg}) \quad (\text{Eq. 5.1})$$

$$1241 \quad J_{V,P_{\gg}} [\text{nmol}\cdot\text{s}^{-1}\cdot\text{L}^{-1}] = J_{V,O_2}\cdot(P_{\gg}/O_2) \quad (\text{Eq. 5.2})$$

1242 We consider isolated mitochondria as powerhouses and proton pumps as molecular machines
 1243 to relate experimental results to energy metabolism of the intact cell. The cellular P \gg /O₂ based
 1244 on oxidation of glycogen is increased by the glycolytic (fermentative) substrate-level
 1245 phosphorylation of 3 P \gg /Glyc, *i.e.*, 0.5 mol P \gg for each mol O₂ consumed in the complete
 1246 oxidation of a mol glycosyl unit (Glyc). Adding 0.5 to the mitochondrial P \gg /O₂ ratio of 5.4
 1247 yields a bioenergetic cell physiological P \gg /O₂ ratio close to 6. Two NADH equivalents are
 1248 formed during glycolysis and transported from the cytosol into the mitochondrial matrix, either
 1249 by the malate-aspartate shuttle or by the glycerophosphate shuttle resulting in different
 1250 theoretical yield of ATP generated by mitochondria, the energetic cost of which potentially
 1251 must be taken into account. Considering also substrate-level phosphorylation in the TCA cycle,
 1252 this high P \gg /O₂ ratio not only reflects proton translocation and OXPHOS studied in isolation,
 1253 but integrates mitochondrial physiology with energy transformation in the living cell (Gnaiger
 1254 1993a).

1255

1256 **5. Conclusions**

1257 MitoEAGLE can serve as a gateway to better diagnose mitochondrial respiratory defects
 1258 linked to genetic variation, age-related health risks, sex-specific mitochondrial performance,
 1259 lifestyle with its effects on degenerative diseases, and thermal and chemical environment. The
 1260 present recommendations on coupling control states and rates, linked to the concept of the
 1261 protonmotive force (Part 1) will be extended in a series of reports on pathway control of

1262 mitochondrial respiration, respiratory states in intact cells, and harmonization of experimental
1263 procedures.

1264

1265 **Box 5: Mitochondrial and cell respiration**

1266 Mitochondrial and cell respiration is the process of highly exergonic and exothermic energy
1267 transformation in which scalar redox reactions are coupled to vectorial ion translocation across
1268 a semipermeable membrane, which separates the small volume of a bacterial cell or
1269 mitochondrion from the larger volume of its surroundings. The electrochemical exergy can be
1270 partially conserved in the phosphorylation of ADP to ATP or in ion pumping, or dissipated in
1271 an electrochemical short-circuit. Respiration is thus clearly distinguished from fermentation as
1272 the counterpart of cellular core energy metabolism. Respiration is separated in mitochondrial
1273 preparations from the partial contribution of fermentative pathways of the intact cell. According
1274 to this definition, residual oxygen consumption, as measured after inhibition of mitochondrial
1275 electron transfer, does not belong to the class of catabolic reactions and is, therefore, subtracted
1276 from total oxygen consumption to obtain baseline-corrected respiration.

1277

1278 The optimal choice for expressing mitochondrial and cell respiration (**Box 5**) as O₂ flow
1279 per biological system, and normalization for specific tissue-markers (volume, mass, protein)
1280 and mitochondrial markers (volume, protein, content, mtDNA, activity of marker enzymes,
1281 respiratory reference state) is guided by the scientific question. Interpretation of the obtained
1282 data depends critically on appropriate normalization, and therefore reporting rates merely as
1283 nmol·s⁻¹ is discouraged, since it restricts the analysis to intra-experimental comparison of
1284 relative (qualitative) differences. Expressing O₂ consumption per cell may not be possible when
1285 dealing with tissues. For studies with mitochondrial preparations, we recommend that
1286 normalizations be provided as far as possible: (1) on a per cell basis as O₂ flow (a biophysical
1287 normalization); (2) per g cell or tissue protein, or per cell or tissue mass as mass-specific O₂

1288 flux (a cellular normalization); and (3) per mitochondrial marker as mt-specific flux (a
1289 mitochondrial normalization). With information on cell size and the use of multiple
1290 normalizations, maximum potential information is available (Renner *et al.* 2003; Wagner *et al.*
1291 2011; Gnaiger 2014). When using isolated mitochondria, mitochondrial protein is a frequently
1292 applied mitochondrial marker, the use of which is basically restricted to isolated mitochondria.
1293 Mitochondrial markers, such as citrate synthase activity as an enzymatic matrix marker, provide
1294 a link to the tissue of origin on the basis of calculating the mitochondrial yield, *i.e.*, the fraction
1295 of mitochondrial marker obtained from a unit mass of tissue.

1296

1297 **Acknowledgements**

1298 We thank M. Beno for management assistance. Supported by COST Action CA15203
1299 MitoEAGLE and K-Regio project MitoFit (EG).

1300 **Competing financial interests:** E.G. is founder and CEO of Oroboros Instruments, Innsbruck,
1301 Austria.

1302

1303 **6. References** (*incomplete; www links will be deleted in the final version*)

1304 Altmann R. Die Elementarorganismen und ihre Beziehungen zu den Zellen. Zweite vermehrte
1305 Auflage. Verlag Von Veit & Comp, Leipzig 1894;160 pp. -

1306 www.mitoeagle.org/index.php/Altmann_1894_Verlag_Von_Veit_%26_Comp

1307 Birkedal R, Laasmaa M, Vendelin M. The location of energetic compartments affects
1308 energetic communication in cardiomyocytes. *Front Physiol* 2014;5:376. doi:

1309 10.3389/fphys.2014.00376. eCollection 2014. PMID: 25324784

1310 **Breton et al. 2007 Trends in Genetics**

1311 Brown GC. Control of respiration and ATP synthesis in mammalian mitochondria and cells.

1312 *Biochem J* 1992;284:1-13. - www.mitoeagle.org/index.php/Brown_1992_Biochem_J

- 1313 Chance B, Williams GR. Respiratory enzymes in oxidative phosphorylation: III. The steady
1314 state. J Biol Chem 1955;217:409-27. -
1315 www.mitoeagle.org/index.php/Chance_1955_J_Biol_Chem-III
- 1316 Chance B, Williams GR. Respiratory enzymes in oxidative phosphorylation. IV. The
1317 respiratory chain. J Biol Chem 1955;217:429-38. -
1318 www.mitoeagle.org/index.php/Chance_1955_J_Biol_Chem-IV
- 1319 Chance B, Williams GR. The respiratory chain and oxidative phosphorylation. Adv Enzymol
1320 Relat Subj Biochem 1956;17:65-134. -
1321 www.mitoeagle.org/index.php/Chance_1956_Adv_Enzymol_Relat_Subj_Biochem
- 1322 Cohen ER, Cvitas T, Frey JG, Holmström B, Kuchitsu K, Marquardt R, Mills I, Pavese F,
1323 Quack M, Stohner J, Strauss HL, Takami M, Thor HL. Quantities, units and symbols in
1324 physical chemistry, IUPAC Green Book 2008;3rd Edition, 2nd Printing, IUPAC & RSC
1325 Publishing, Cambridge. -
1326 www.mitoeagle.org/index.php/Cohen_2008_IUPAC_Green_Book
- 1327 Coopersmith J. Energy, the subtle concept. The discovery of Feynman's blocks from Leibnitz
1328 to Einstein. Oxford University Press 2010;400 pp.
- 1329 Dai Q, Shah AA, Garde RV, Yonish BA, Zhang L, Medvitz NA, Miller SE, Hansen EL, Dunn
1330 CN, Price TM. A truncated progesterone receptor (PR-M) localizes to the
1331 mitochondrion and controls cellular respiration. ???
- 1332 Dufour S, Rousse N, Canioni P, Diolez P. Top-down control analysis of temperature effect on
1333 oxidative phosphorylation. Biochem J 1996;314:743-51.
- 1334 Ernster L, Schatz G Mitochondria: a historical review. J Cell Biol 1981;91:227s-55s. -
1335 www.mitoeagle.org/index.php/Ernster_1981_J_Cell_Biol
- 1336 Estabrook RW. Mitochondrial respiratory control and the polarographic measurement of
1337 ADP:O ratios. Methods Enzymol 1967;10:41-7. -
1338 www.mitoeagle.org/index.php/Estabrook_1967_Methods_Enzymol

- 1339 Fell D. Understanding the control of metabolism. Portland Press 1997.
- 1340 Garlid KD, Semrad C, Zinchenko V. Does redox slip contribute significantly to mitochondrial
1341 respiration? In: Schuster S, Rigoulet M, Ouhabi R, Mazat J-P (eds) Modern trends in
1342 biothermokinetics. Plenum Press, New York, London 1993;287-93.
- 1343 Gerö D, Szabo C. Glucocorticoids suppress mitochondrial oxidant production via
1344 upregulation of uncoupling protein 2 in hyperglycemic endothelial cells. PLoS One
1345 2016;11:e0154813.
- 1346 Gnaiger E. Efficiency and power strategies under hypoxia. Is low efficiency at high glycolytic
1347 ATP production a paradox? In: Surviving Hypoxia: Mechanisms of Control and
1348 Adaptation. Hochachka PW, Lutz PL, Sick T, Rosenthal M, Van den Thillart G (eds.)
1349 CRC Press, Boca Raton, Ann Arbor, London, Tokyo 1993a:77-109. -
1350 www.mitoeagle.org/index.php/Gnaiger_1993_Hypoxia
- 1351 Gnaiger E. Nonequilibrium thermodynamics of energy transformations. Pure Appl Chem
1352 1993b;65:1983-2002. - www.mitoeagle.org/index.php/Gnaiger_1993_Pure_Appl_Chem
- 1353 Gnaiger E. Bioenergetics at low oxygen: dependence of respiration and phosphorylation on
1354 oxygen and adenosine diphosphate supply. Respir Physiol 2001;128:277-97. -
1355 www.mitoeagle.org/index.php/Gnaiger_2001_Respir_Physiol
- 1356 Gnaiger E. Mitochondrial pathways and respiratory control. An introduction to OXPHOS
1357 analysis. 4th ed. Mitochondr Physiol Network 2014;19.12. Oroboros MiPNet
1358 Publications, Innsbruck:80 pp. -
1359 www.mitoeagle.org/index.php/Gnaiger_2014_MitoPathways
- 1360 Gnaiger E. Capacity of oxidative phosphorylation in human skeletal muscle. New
1361 perspectives of mitochondrial physiology. Int J Biochem Cell Biol 2009;41:1837-45. -
1362 www.mitoeagle.org/index.php/Gnaiger_2009_Int_J_Biochem_Cell_Biol
- 1363 Gnaiger E, Méndez G, Hand SC. High phosphorylation efficiency and depression of
1364 uncoupled respiration in mitochondria under hypoxia. Proc Natl Acad Sci USA

- 1365 2000;97:11080-5. -
- 1366 www.mitoeagle.org/index.php/Gnaiger_2000_Proc_Natl_Acad_Sci_U_S_A
- 1367 Hofstadter DR. Gödel, Escher, Bach: An eternal golden braid. A metaphorical fugue on minds
1368 and machines in the spirit of Lewis Carroll. Harvester Press 1979;499 pp. -
- 1369 www.mitoeagle.org/index.php/Hofstadter_1979_Harvester_Press
- 1370 Illaste A, Laasmaa M, Peterson P, Vendelin M. Analysis of molecular movement reveals
1371 latticelike obstructions to diffusion in heart muscle cells. *Biophys J* 2012;102:739-48. -
- 1372 PMID: 22385844
- 1373 Jepihhina N, Beraud N, Sepp M, Birkedal R, Vendelin M. Permeabilized rat cardiomyocyte
1374 response demonstrates intracellular origin of diffusion obstacles. *Biophys J*
1375 2011;101:2112-21. - PMID: 22067148
- 1376 Komlódi T, Tretter L. Methylene blue stimulates substrate-level phosphorylation catalysed by
1377 succinyl-CoA ligase in the citric acid cycle. *Neuropharmacology* 2017;123:287-98. -
- 1378 www.mitoeagle.org/index.php/Komlodi_2017_Neuropharmacology
- 1379 Lee SR, Kim HK, Song IS, Youm J, Dizon LA, Jeong SH, Ko TH, Heo HJ, Ko KS, Rhee BD,
1380 Kim N, Han J. Glucocorticoids and their receptors: insights into specific roles in
1381 mitochondria. *Prog Biophys Mol Biol* 2013;112:44-54.
- 1382 Lemieux H, Blier PU, Gnaiger E. Remodeling pathway control of mitochondrial respiratory
1383 capacity by temperature in mouse heart: electron flow through the Q-junction in
1384 permeabilized fibers. *Sci Rep* 2017;7:2840. -
- 1385 www.mitoeagle.org/index.php/Lemieux_2017_Sci_Rep
- 1386 Lenaz G, Tioli G, Falasca AI, Genova ML. Respiratory supercomplexes in mitochondria. In:
1387 Mechanisms of primary energy trasduction in biology. M Wikstrom (ed) Royal Society
1388 of Chemistry Publishing, London, UK 2017:296-337 (in press)
- 1389 Margulis L. Origin of eukaryotic cells. New Haven: Yale University Press 1970.

- 1390 Meinild Lundby AK, Jacobs RA, Gehrig S, de Leur J, Hauser M, Bonne TC, Flück D,
1391 Dandanell S, Kirk N, Kaech A, Ziegler U, Larsen S, Lundby C. Exercise training
1392 increases skeletal muscle mitochondrial volume density by enlargement of existing
1393 mitochondria and not de novo biogenesis. *Acta Physiol (Oxf)* 2017;[Epub ahead of
1394 print].
- 1395 Miller GA. *The science of words*. Scientific American Library New York 1991;276 pp. -
1396 www.mitoeagle.org/index.php/Miller_1991_Scientific_American_Library
- 1397 Mitchell P. Chemiosmotic coupling in oxidative and photosynthetic phosphorylation *Biochim*
1398 *Biophys Acta Bioenergetics* 2011;1807:1507-38. -
1399 <http://www.sciencedirect.com/science/article/pii/S0005272811002283>
- 1400 Mitchell P, Moyle J. Respiration-driven proton translocation in rat liver mitochondria.
1401 *Biochem J* 1967;105:1147-62. -
1402 www.mitoeagle.org/index.php/Mitchell_1967_Biochem_J
- 1403 Moreno M, Giacco A, Di Munno C, Goglia F. Direct and rapid effects of 3,5-diiodo-L-
1404 thyronine (T2). *Mol Cell Endocrinol* 2017;7207:30092-8.
- 1405 Morrow RM, Picard M, Derbeneva O, Leipzig J, McManus MJ, Gousspillou G, Barbat-Artigas
1406 S, Dos Santos C, Hepple RT, Murdock DG, Wallace DC. Mitochondrial energy
1407 deficiency leads to hyperproliferation of skeletal muscle mitochondria and enhanced
1408 insulin sensitivity. *Proc Natl Acad Sci U S A* 2017;114:2705-10. -
1409 www.mitoeagle.org/index.php/Morrow_2017_Proc_Natl_Acad_Sci_U_S_A
- 1410 Nicholls DG, Ferguson S. *Bioenergetics 4*. Elsevier 2013.
- 1411 Paradies G, Paradies V, De Benedictis V, Ruggiero FM, Petrosillo G. Functional role of
1412 cardiolipin in mitochondrial bioenergetics. *Biochim Biophys Acta* 2014;1837:408-17. -
1413 http://www.mitoeagle.org/index.php/Paradies_2014_Biochim_Biophys_Acta
- 1414 Price TM, Dai Q. The Role of a Mitochondrial Progesterone Receptor (PR-M) in
1415 Progesterone Action. *Semin Reprod Med.* 2015;33:185-94.

- 1416 Prigogine I. Introduction to thermodynamics of irreversible processes. Interscience, New
1417 York, 1967;3rd ed.
- 1418 Puchowicz MA, Varnes ME, Cohen BH, Friedman NR, Kerr DS, Hoppel CL. Oxidative
1419 phosphorylation analysis: assessing the integrated functional activity of human skeletal
1420 muscle mitochondria – case studies. *Mitochondrion* 2004;4:377-85. -
1421 www.mitoeagle.org/index.php/Puchowicz_2004_Mitochondrion
- 1422 P. M. Quiros, A. Mottis, and J. Auwerx. Mitonuclear communication in homeostasis and
1423 stress. *Nat Rev Mol Cell Biol* 2016;17:213-26.
- 1424 Renner K, Amberger A, Konwalinka G, Gnaiger E. Changes of mitochondrial respiration,
1425 mitochondrial content and cell size after induction of apoptosis in leukemia cells.
1426 *Biochim Biophys Acta* 2003;1642:115-23. -
1427 www.mitoeagle.org/index.php/Renner_2003_Biochim_Biophys_Acta
- 1428 Rich P. Chemiosmotic coupling: The cost of living. *Nature* 2003;421:583. -
1429 www.mitoeagle.org/index.php/Rich_2003_Nature
- 1430 Rostovtseva TK, Sheldon KL, Hassanzadeh E, Monge C, Saks V, Bezrukov SM, Sackett DL.
1431 Tubulin binding blocks mitochondrial voltage-dependent anion channel and regulates
1432 respiration. *Proc Natl Acad Sci USA* 2008;105:18746-51. -
1433 www.mitoeagle.org/index.php/Rostovtseva_2008_Proc_Natl_Acad_Sci_U_S_A
- 1434 Rustin P, Parfait B, Chretien D, Bourgeron T, Djouadi F, Bastin J, Rötig A, Munnich A.
1435 Fluxes of nicotinamide adenine dinucleotides through mitochondrial membranes in
1436 human cultured cells. *J Biol Chem* 1996;271:14785-90.
- 1437 Saks VA, Veksler VI, Kuznetsov AV, Kay L, Sikk P, Tiivel T, Tranqui L, Olivares J, Winkler
1438 K, Wiedemann F, Kunz WS. Permeabilised cell and skinned fiber techniques in studies
1439 of mitochondrial function in vivo. *Mol Cell Biochem* 1998;184:81-100. -
1440 http://www.mitoeagle.org/index.php/Saks_1998_Mol_Cell_Biochem

- 1441 Salabei JK, Gibb AA, Hill BG. Comprehensive measurement of respiratory activity in
1442 permeabilized cells using extracellular flux analysis. *Nat Protoc* 2014;9:421-38.
- 1443 Sazanov LA. A giant molecular proton pump: structure and mechanism of respiratory
1444 complex I. *Nat Rev Mol Cell Biol* 2015;16:375-88. -
1445 www.mitoeagle.org/index.php/Sazanov_2015_Nat_Rev_Mol_Cell_Biol
- 1446 Schönfeld P, Dymkowska D, Wojtczak L. Acyl-CoA-induced generation of reactive oxygen
1447 species in mitochondrial preparations is due to the presence of peroxisomes. *Free Radic*
1448 *Biol Med* 2009;47:503-9.
- 1449 Schrödinger E. *What is life? The physical aspect of the living cell.* Cambridge Univ Press,
1450 1944. - www.mitoeagle.org/index.php/Gnaiger_1994_BTK
- 1451 Simson P, Jepihhina N, Laasmaa M, Peterson P, Birkedal R, Vendelin M. Restricted ADP
1452 movement in cardiomyocytes: Cytosolic diffusion obstacles are complemented with a
1453 small number of open mitochondrial voltage-dependent anion channels. *J Mol Cell*
1454 *Cardiol* 2016;97:197-203. - PMID: 27261153
- 1455 Stucki JW, Ineichen EA. Energy dissipation by calcium recycling and the efficiency of
1456 calcium transport in rat-liver mitochondria. *Eur J Biochem* 1974;48:365-75.
- 1457 Wagner BA, Venkataraman S, Buettner GR. The rate of oxygen utilization by cells. *Free*
1458 *Radic Biol Med.* 2011;51:700-712.
1459 <http://dx.doi.org/10.1016/j.freeradbiomed.2011.05.024> PMID: PMC3147247
- 1460 Watt IN, Montgomery MG, Runswick MJ, Leslie AG, Walker JE. Bioenergetic cost of
1461 making an adenosine triphosphate molecule in animal mitochondria. *Proc Natl Acad Sci*
1462 *U S A* 2010;107:16823-7. -
1463 www.mitoeagle.org/index.php/Watt_2010_Proc_Natl_Acad_Sci_U_S_A
- 1464 Weibel ER, Hoppeler H. Exercise-induced maximal metabolic rate scales with muscle aerobic
1465 capacity. *J Exp Biol* 2005;208:1635-44.

- 1466 Wikström M, Hummer G. Stoichiometry of proton translocation by respiratory complex I and
1467 its mechanistic implications. Proc Natl Acad Sci U S A 2012;109:4431-6. -
1468 www.mitoeagle.org/index.php/Wikstroem_2012_Proc_Natl_Acad_Sci_U_S_A
1469 Willis WT, Jackman MR, Messer JI, Kuzmiak-Glancy S, Glancy B. A simple hydraulic
1470 analog model of oxidative phosphorylation. Med Sci Sports Exerc. 2016;48:990-1000.